

**Study on the Development of Electrochemical Microdevice for  
the Detection of Organophosphate Pesticides**

**May 2015**

**Jin WANG**

**Study on the Development of Electrochemical Microdevice for  
the Detection of Organophosphate Pesticides**

A Dissertation Submitted to  
the Graduate School of Life and Environmental Sciences,  
the University of Tsukuba  
in Partial Fulfillment of the Requirements  
for the Degree of Doctor of Philosophy in Biotechnology  
(Doctoral Program in Bioindustrial Sciences)

**Jin WANG**

# CONTENTS

	Page
<b>CONTENTS</b> .....	i
<b>LIST OF TABLES</b> .....	iv
<b>LIST OF FIGURES</b> .....	v
<b>ABSTRACT</b> .....	viii
<b>CHAPTER 1 General Introduction</b> .....	1
1.1 General introduction.....	1
1.1.1 Pesticides in agriculture.....	1
1.1.2 Detection technique for pesticides.....	3
1.1.3 Microfabrication technique.....	9
1.2 Objectives of this study .....	11
<b>REFERENCES</b> .....	19
<b>CHAPTER 2 Microfluidic Device for Coulometric Detection of Organophosphate</b>	
<b>Pesticides based on Acetylcholinesterase Inhibition</b> .....	21
2.1 Introduction .....	21
2.2 Experimental section .....	23
2.2.1 Reagents and materials .....	23
2.2.2 Device fabrication.....	24
2.2.3 On-chip processing of liquid plugs.....	34
2.2.4 Principles underlying coulometric detection of OPs .....	36

2.2.5 Measurement procedure.....	37
2.3 Results and Discussion.....	38
2.3.1. Coulometric detection of H <sub>2</sub> O <sub>2</sub> and the stability of the microfabricated device ...	38
2.3.2 Detection of OPs by AChE inhibition .....	40
2.3.3 Influence of organic solvents.....	43
2.3.5 Temperature dependence .....	47
2.3.6 Detection of malathion using the device .....	48
2.4 Conclusions .....	51
<b>REFERENCES</b> .....	52
<b>CHAPTER 3 Microfabricated pH Sensing Device for the Direct Determination of</b>	
<b>Organophosphate Pesticide .....</b>	<b>56</b>
3.1 Introduction .....	56
3.2 Materials and methods .....	57
3.2.1 Reagents and materials .....	57
3.2.2 Device fabrication.....	57
3.2.3 Measurement procedure.....	67
3.3 Results and Discussion.....	67
3.3.1 Performance characterization of the IrOx electrode .....	67
3.3.2 Potentiometric determination of diazinon .....	70
3.4 Conclusions .....	76
<b>REFERENCES</b> .....	77
<b>CHAPTER 4 Overall Conclusions .....</b>	<b>80</b>
<b>ACKNOWLEDGEMENTS</b> .....	<b>84</b>

**APPENDIX** ..... 85

## LIST OF TABLES

	Page
Table 1.1 Organophosphates included in the OP Cumulative Assessment.....	12
Table 1.2 Properties of Controlled-Potential Techniques .....	13
Table 1.3 Screen-printed enzymatic biosensors for pesticides detection.....	14
Table 1.4 Principal methods for enzyme immobilization in biosensors .....	15
Table 1.5 Examples of potentiometric transducers biosensors.....	16
Table 1.6 Examples of bi-enzyme amperometric biosensors.....	17
Table 1.7 The lowest detection limit for pesticides detection with enzymatic .....	18
electrochemical biosensors.....	18
Table 2.1 Charge measured accompanying the enzymatic reactions at different .....	47
temperature. ATCh concentration: 2 mM. Each point in the graph.....	47
represents the average of three measurements. Standard deviations are also	
shown. ....	47
Table 2. 2 Summary of Current International Tolerances and Maximum Residue	
Limits (ppm).....	50
Table 3.1 Response of the potentiometric electrode to other pesticides .....	73
Table 3.2 Limit of direct detection of OP biosensors for various OPs. ....	75

## LIST OF FIGURES

	Page
Fig. 2.1 The fabricated device. A: Exploded view of the device. B: The device on a finger Planar dimensions are 30 mm × 11 mm... ..	26
Fig. 2.2 Schematic illustration of the fabrication of on chip electrode for coulometric device. ....	31
Fig. 2.3 Schematic illustration formation of Ag/AgCl layer on the device. ....	32
Fig. 2.4 Steps in processing plugs of solutions. (a) A substrate solution and a solution containing enzymes and an OP were introduced into the main flow channel. (b-d) The volume of each plug was measured using the auxiliary flow channel and the parts of the plugs in the main flow channel were discarded (e) The two plug solutions were merged in the main flow channel (f) The new plug was transported to the sensing region and the components were mixed... ..	35
Fig. 2.5 Dependence of charges on the concentration of H <sub>2</sub> O <sub>2</sub> . The inset shows the plot at lower H <sub>2</sub> O <sub>2</sub> concentrations. Each data point represents the average of three measurements; averages and standard deviations are shown. ....	39
Fig. 2.6 Reproducibility of the output charge obtained with 100 mM H <sub>2</sub> O <sub>2</sub> . ....	40
Fig. 2.7 Charge measured accompanying the enzymatic reactions in the presence of 100 μM OP after pre-incubation for various time. Each data point represents the average of three measurements; averages and standard deviations are shown. ....	42
Fig. 2.8 Calibration plots obtained for commercial formulations of OPs. Each data point represents the average of three measurements; averages and standard deviations are shown. ....	43

Fig. 2.9 Inhibition of AChE after 8-min incubation in 5–40% polar organic solvents. The inset shows data obtained using pure organic solvents. Each data point represents the average of three measurements; averages and standard deviations are shown. ....	44
Fig. 2.10 The influence of the substrate (ATCh) on final charge. A: Dependence of the generated charge on the concentration of ATCh. The symbols correspond to three measurements B: Calibration plot for the device obtained by successive additions of the substrate. ....	46
Fig. 2.11 Dependence of AChE inhibition on the concentration of malathion. Each point in the graph represents the average and standard deviations of three measurements. ....	49
Fig. 3.1 Construction of the device. A: Exploded view of the device. B: Top view showing the mutual relation between the structures of the layers. C: Cross-section along the line X-X' in A. D: The device on a finger. Planar dimensions are 20 mm × 11 mm. ....	63
Fig. 3.2 Schematic illustration of the fabrication of on chip electrode for pH-sensing device. ....	64
Fig. 3.3 Schematic illustration formation of Ag/AgCl layer on the device. ....	65
Fig. 3.4 Formation of Ir/IrO <sub>x</sub> layer for pH-sensing device. ....	66
Fig. 3.5 Calibration plot for the IrO <sub>x</sub> pH electrode obtained using the on-chip liquid junction Ag/AgCl reference electrode. Eight measurements were done for each point, and averages and standard deviations are shown. All of the error bars are behind the symbols. ....	68



Fig. 3.6 Stability of the IrO <sub>x</sub> electrode in solutions of different pH values. Each data point represents the average of four measurements; averages and standard deviations are shown. Most of the error bars are behind the symbols. ....	69
Fig. 3.7 Response curves of the IrO <sub>x</sub> electrode to pH changes. A: Adding a NaOH solution to a HCl solution (pH 1.6), B: adding a HCl solution to a NaOH solution (pH 13.9). ....	70
Fig. 3.8 Response of starting buffer pH on PON1 electrode to 0.1 mM diazinon. ....	71
Fig. 3.9 Reproducibility of the PON 1 IrO <sub>x</sub> electrode at 0.1 mM diazinon.....	72
Fig. 3.10 Calibration plots for organophosphate pesticide (diazinon). ....	74

## ABSTRACT

Organophosphate pesticides (OPs) are the most widely used in agriculture and environment. In U.S., OPs were genetically explored in crops like corn, which is the backbone of the U.S. food system in many ways as high-fructose corn syrup, cattle feed, and a large variety of other processed food product, playing a major role in dietary risk exposure in the U.S. OPs are hazardous and acute toxic for food safety, public health and environmental issues since organophosphate pesticides can irreversibly inactivate acetylcholinesterase (AChE), which is essential to nerve impulses in insects, many other animals, and human beings. Currently used conventional methods are powerful for detecting trace levels of OPs but suffered some disadvantages such as they are time-consuming, expensive and require highly trained personnel. With the recent progress in the development of micro-total systems ( $\mu$ TAS) or Lab-on-a-Chip technologies, microfluidics have been proposed as a promising technique for organophosphate pesticides detection coupled with analytical electrochemistry. Therefore, in this study, the microfabricated device based on analytical electrochemistry were developed and applied for organophosphate pesticides detection.

In the first chapter, the general introduction of the organophosphate pesticides, analytical electrochemistry and microfabrication were summarized. Moreover, this part also reviewed the former researches in the areas of organophosphate pesticides detection, main technologies, the development and application of analytical electrochemistry chip device on determination of organophosphate pesticides as well as other field.

In the second chapter, a coulometric microdevice based on plug-based microfluidics was developed for the detection of organophosphate pesticides. Detection was based on the inhibition of an enzyme, acetylcholinesterase (AChE), by the OPs. Microfabrication technique was used for fabrication of coulometric device. The microfabrication procedure

including design and fabrication process was described in detail. Hydrogen peroxide ( $\text{H}_2\text{O}_2$ ), produced in a series of enzymatic reactions involving AChE and choline oxidase (ChOx), was oxidized on a microelectrode array, and changes in AChE activity upon addition of an OP were measured by coulometry. A linear relationship was confirmed between the charge generated and the logarithm of the OP concentration. The lower limit of detection (LOD) was 33 nM for malathion and 90 nM for acephate, MEP, and diazinon. An increase in the ratio of organic solvents was also found to inhibit AChE activity. However, the concentrations sufficient to produce this effect were several orders of magnitude higher than those of the OPs, indicating that this influence can be ignored in the analysis of OPs.

To solve the problems of formation and manipulation of plugs containing the two enzymes difficult in PDMS flow channels and the cost of use of the two enzymes in the reactions, a mono-enzyme system was used. Thiocholine (TCh) produced in the enzymatic reaction of AChE with acetylthiocholine (ATCh) as a substrate was oxidized on a microelectrode array formed in a main flow channel. Volumes of plugs of necessary solutions were measured using a structure consisting of a row of rhombuses formed in an auxiliary flow channel. The plugs were merged and solution components were mixed at a T-junction formed with the main and auxiliary flow channels. A linear relationship was confirmed between the generated charge and the logarithm of the OP (malathion) concentration in a concentration range between  $10^{-6}$  M and  $10^{-3}$  M with a correlation coefficient of 0.951. The lower limit of detection was 412 nM.

In the second chapter, the OPs detection is indirect. But in the third chapter, an  $\text{IrO}_x$  pH sensor was used for direct determination of organophosphate pesticides (OPs). Detection was based on the sensing of a pH change accompanying the enzymatic hydrolysis of OPs. Paraoxonase 1 (PON1) was used to catalyze the hydrolysis of OPs to release protons, the

concentration of which is proportional to the amount of OPs. The presence of OPs can be observed as potential change in the IrO<sub>x</sub> pH-sensing electrode. When diazinon was used as a model OP, the lower limit of detection was 2.5 μM. Consumption of solutions was on the order of μL. Low cost and simple detection make the micro potentiometric sensor useful for various applications.

## CHAPTER 1

### General Introduction

#### 1.1 General introduction

##### 1.1.1 Pesticides in agriculture

Pesticides, mainly refer to insecticides, herbicides, fungicides and various other chemical warfare, which are intended for preventing or destroying any pest that hazardous to agricultural product. They can destroy the disease, control insects and other pests. Farmers take advantage of variety of practices or regulations to reduce yield losses to pests by determine which and when pesticides might be used. Meanwhile, pesticides could also do harm to humans, animals and the environment by their very nature because they can kill or affect living organisms. During those pesticides, organophosphate pesticides (OPs) are the widely used since they are discovered in 1932 and developed in the early 19<sup>th</sup> century. According to the database of EPA, the amount of pesticide used in 2006 and 2007 totaled about 821 and 857 million pounds and the top five organophosphate used in 2007 are chlorpyrifos, malathion, acephate, naled, dicotophos. Besides, the amount has reduced from 70% in 1990 to 36% in 2007.

Organophosphate Pesticides (OPs), a group of organophosphates compounds, are the most widely used in residential landscaping, agriculture, environment, and in public health pest control programs as insecticides or nerve agents. Some hypertoxic OPs, such as ethyl parathion and diazinon, have been banned or severely restricted by the United States Environmental Protection Agency (US EPA) with large amounts were used in agricultural spraying on fruits and vegetables and residential settings. Commonly used organophosphate compounds have included malathion, diazinon, parathion, methylparathion, acephate, fenitrothion (MEP), chlorpyrifos, dichlorvos. For instance,

chlorpyrifos and DDT are the most widely used pesticides in U.S. agriculture with long-lasting persistent organic pollutant (POP) in food chain, and can be found in butter and milk. These are only two of the dozens of pesticides found in our daily food. Even after washing, there are still little residue in food. Organophosphate pesticides can irreversibly inactivate the enzyme acetylcholinesterase (AChE), which is responsible for the transmission of nerve impulses to cholinergic synapses relevant to human memory and Alzheimer's disease. Organophosphate pesticides affect this enzyme by forming covalent bonds to serine residues in the active site of the enzyme AChE, impairing the enzyme function in their potential for poisoning, leading to the cholinergic dysfunction and eventual death. Apparently, washing is unlikely to be helpful. Washed and peeled the samples, some pesticides are taken up by a plant's roots and distributed throughout the plant; so washing will not remove these pesticides, which is also called systemic pesticides, playing a major role in dietary risk exposure in the U.S. According to one analysis, has been on the rise since the last 15 years. Included in systemic pesticides are genetically explored in crops like corn, which is the backbone of the U.S. food system in many ways as high-fructose corn syrup, cattle feed, and a large variety of other processed food product.

Organophosphate pesticides can be hydrolyzed rapidly when exposed to sunlight, air, and soil, although small amounts can be detected in food and drinking water. Even at relatively low-level residual, organophosphates pesticides may also be the most hazardous and acute toxic for food safety, public health and environmental issues. They can be absorbed by eating the vegetables and fruits or through breath or skin contact.

### **1.1.2 Detection technique for pesticides**

Many techniques have been developed for the detection of OPs to improve food safety and public health, and to address environmental concerns. Currently used conventional methods include gas chromatography (GC), high performance liquid chromatography (HPLC), and coupled chromatographic-spectrometric procedures (GC-MS, HPLC-MS). These techniques are very powerful for detecting trace levels of OPs. For example, HPLC is suitable to deal with polar compounds than GC since the metabolized product of pesticide is more polar. Besides, HPLC can analyze both the parent and metabolized product at the same time. Take the recent examples that HPLC was used for fungicide, insecticide, and herbicide.

The Table 1.1 shows the US EPA's review of individual OPs has resulted in the issuance of Interim Reregistration Eligibility Decisions (IREDs) for 22 OPs, interim Tolerance Reassessment and Risk Management Decisions (TREDs) for 8 OPs, and a Reregistration Eligibility Decision (RED) for one OP, malathion.

Electrochemistry technique, which combines electricity and chemistry, building the relationship between electrical (signal current, potential, or charge) and chemical parameters, play an important role in electrical measurement for analytical purposes for various applications including food and water quality control, environment monitoring, or biomedical analysis. The developments of microelectrodes, the microfabrication and microfluidics have made the electroanalysis popular and led to an industrial increase. Furthermore, it is expanded into new fields and environments. Evidently, analytical electrochemistry is gaining a major attention and application in the development of chemical sensors and biosensors.

The electrochemical process occurs at the interface between the electrode and solution, which is none like other many chemical measurements that involve homogeneous solutions.

The electroanalytical measurements can be divided into two principal types based on the type of electrical signal used for the quantitation. One is potentiometric and the other is potentiostatic. Both types need at least two electrodes and a connecting electrolyte solution, which establish the electrochemical cell. Therefore, the surface of the electrode is a junction between an ionic and electronic conductor. One of the two electrodes is termed the working (or indicator) electrode and the second electrode is termed the reference electrode.

Potentiometry is a zero-current (static) technique and the measurement is conducted during the potential established across a membrane. There are many different types of membrane materials for processing different ion recognition and determination with high selectivity, which has been widely used for monitoring ionic such as protons, potassium and calcium ions in solution samples.

Potentiostatic, also called controlled - potential, is a technique for monitoring charge transfer at the interface of electrode – solution based on dynamic (non-zero-current) situations. The electrode potential is used for separating an electron transfer reaction and the resultant current is measured. The electrode potential (electron pressure) applied forced the chemical reaction to gain or lost electron (reduction or oxidation); on the other hand, the resulting current was formed and measured when electron moves across the electrode – solution interface. The potentiostatic technique has various advantages including high sensitivity, a wide linear range, portable and low-cost device that allow various unusual situations and environments. Table 1.2 summarized several properties of the potentiostatic technique.

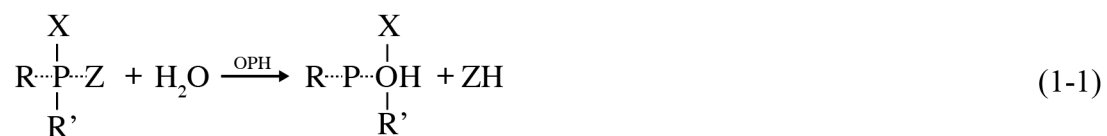
In the last two decades, electrochemical biosensors have significantly increased and become an important tool for organophosphate pesticides. These electrochemical biosensors have tremendous advantages over the classical methods currently used in



analytical chemistry laboratory (gas chromatography and high performance liquid chromatography) including high sensitivity, high specificity, rapid response, relatively compact size with low cost and easy to operation that are able to gain the real-time qualitative and quantitative information about the target analytes with minimum sample preparation and consumption. Because of these excellent performances, the electrochemical biosensors provide a reliable alternative to the conventional methods.

Those numerous electrochemical biosensors, mainly refer to enzymatic biosensors, which are developed by using various electrochemical signal transducer and various measuring methods based on enzymatic inhibition of the activity of enzymes including acetylcholinesterase (AChE), butyrylcholinesterase (BChE), organophosphate hydrolase (OPH), aldehyde dehydrogenase (ADH), acid phosphatase (AP) and Tyrosinase for organophosphate pesticides detection. Accordingly, the enzymatic biosensors can be divided into two categories: enzymatic biosensors for direct detection of organophosphate pesticides and biosensors based on enzyme activity inhibition. The Table 1.3 is the list of reported screen-printed enzymatic biosensors for pesticides detection.

For the first category, enzymatic biosensor for direct detection of OPs, Aryldialkylphosphatase enzymes have been used such as organophosphate hydrolase (OPH), parathion hydrolase, organophosphorus acid hydrolase (OPAA) phosphotriesterase, and paraoxon hydrolase. Aryldialkylphosphatase is an enzyme that hydrolyzes organophosphates. The enzyme has wide substrate specificity and can hydrolyze many OPs such as diazinon, paraoxon, parathion, methyl parathion and sarin, soman. For OPH, as shown in the following equation:

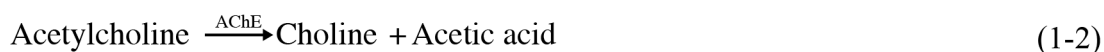


During the hydrolysis of organophosphate compounds, release of protons was monitored for construction of potentiometric biosensors. Usually, the pH changes were measured by potentiometric biosensors with pH enzyme electrode, glass pH electrode, pH-sensitive field effect transistors and screen-printed H<sup>+</sup>-sensitive layer. Another measurement was based on the rapid oxidation signal of p-nitrophenol at the OPH/Nafion layer immobilized on the printed carbon surface determined by amperometric biosensors. The parathion detection is also based on amperometric detection of p-nitrophenol with screen-printed biosensors with immobilized parathion hydrolase (OP). A. Mulchandain et al. (2001) reported a simple pH electrode, which was modified with an immobilized OPH layer, formed by cross-linking OPH with bovine serum albumin and glutaraldehyde for direct determination of organophosphate pesticides. The group also immobilized organophosphorus acid anhydrolase (OPAA) for the same purpose. Furthermore, they developed two different optical based biosensors based on measurement of the changes in the fluorescence intensity of the fluorescein isothiocyanate (FITC) and the relationship between the amount of OPs hydrolyzed and the amount of chromophoric product during the enzymatic catalyze hydrolysis.

For the second category, this is biosensing based on inhibition of selected enzyme activity, mainly employed for the determination of organophosphate pesticides, which is used much earlier than the first category (direct enzymatic determination) and is more advanced used with various electrochemical biosensors. The mechanism is based on choline esterase enzyme inhibition since organophosphate pesticides can inhibit choline esterase. Acetylcholinesterase (AChE), butyrylcholinesterase (BChE), organophosphate

hydrolase (OPH), aldehyde dehydrogenase (ADH), acid phosphatase (AP) and Tyrosinase were used for this kind of biosensors. Among them, Acetylcholinesterase and butyrylcholinesterase were predominately utilized for indirect enzymatic determinations. The Table 1.4 showed the principal methods for enzyme immobilization in biosensors.

A potentiometric or amperometric signal transducers are commonly used in design of electrochemical biosensors for pesticides detection based on acetylcholinesterase inhibition. For potentiometric transducers can provide a wide range of dependence of signal versus analyte concentration but suffer the slow response time compared with amperometric transducers. The mechanism of potentiometric detection can be summarized in the following equation:

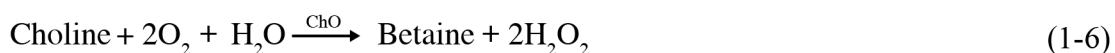


Commonly, the enzyme was immobilized on the surface of a pH glass electrode, Ir/IrOx electrode, and Pd/PdO electrode in various ways including immobilized in the layer of cross-linked polymers or cross-linked bovine serum albumin or other membranes. Tran-Minh et al. (1990) reported a pH glass electrode for paraoxon, malathion and parathion methyl detection with the 1 h incubation time in the range from 0.1 to 1nM. M.N. Hendji et al. (1993) improved the detection limit for DFP (diisopropyl fluorophosphate) at 20 min incubation time as low as  $10^{-12}$  M with freshly prepared biosensor for each measurement. Examples of potentiometric transducers biosensors are list in Table 1.5.

However, a larger number of electrochemical biosensors for pesticide detection based on acetylcholinesterase was developed using amperometric transducers than potentiometric transducers with only immobilized AChE. The final detection signal was measured based on anodic oxidation of thiocholine formed during enzymatic hydrolysis of the substrate acetylthiocholine shown as follows:



Another amperometric detection of pesticides based on acetylcholinesterase is performed by bienzymatic systems (cholinesterases and choline oxidase), in which, the final signal hydrogen peroxide produced by choline oxidized by choline oxidase (ChOx) was detected by amperometry according to the reactions:



Bioenzymatic amperometric detection can be carried out immobilized ChO only or both of enzymes (AChE and ChO). The examples of bi-enzyme amperometric biosensors were shown in Table 1. 6.

Butyrylcholinesterase inhibition determination is employed as frequently as AChE in design of electrochemical biosensors for indirect detection of pesticides. A potentiometric or amperometric detection is also used in design of BChE biosensors for pesticide determination. Potentiometric biosensors detection is based on different electrodes sensitive to pH changes during the reactions described as follows:



S. Kumaran et al. (1992) immobilized the BChE in a metacrylate polymer by cross-linking on nylon membrane and Pall Biodyne membrane with the limit of detection for pesticides in the range from 0.2 to 10 ppm. A. Evtugyn et al (1997) immobilized the BChE on a white tracing paper for testing pollution of municipal and industrial wastes. For amperometric determination, the biosensors are based on anodic detection of thiocholine formed by enzymatic hydrolysis reaction with immobilized BChE. For paraoxon and heptenophos

determination, a cobalt ophthalocyanine modified carbon epoxy electrode and immobilized enzyme on the nylon membrane were proposed with the detection limits 1.5 and 8.4 ppb respectively by P. Skladal et al. (1992). Similar to AChE, BChE bienzymatic biosensors can also be designed for pesticides detection, where choline oxidase was also used. A biosensor with a Pt electrode covered with a nylon membrane with immobilized BChE and ChO were reported with detection of limit 2 ppb for paraoxon and 6 ppb for malathion by L. Campanella et al. (1992). The Table 1.7 showed the lowest detection limit for pesticides detection with enzymatic electrochemical biosensors.

### **1.1.3 Microfabrication technique**

Microfabrication is the fabrication process for miniature structure in micrometer scales and even smaller. These microstructures created by microfabrication technique provide great opportunity to study basic scientific phenomena that taken place at small dimensions. Over the past decade, microfabrication has attracted rapidly growing interest in modern science and technology. Most research in microfabrication has been focused on microelectromechanical systems (MEMS), microsystems, micromachines and their subfields including lab-on-a chip, also known as micro total analysis systems ( $\mu$ TAS), microfluidics, optical MEMS, BioMEMS and extension into nanoscale (NEMS, for nano electro mechanical systmes).

Miniaturized devices present great promising in many areas of science and engineering: chemistry, electrical engineering, materials sciences, and physics. The particularly application of this miniaturized device for microanalytical is in the separation, analysis and synthesis of chemical and biological compounds. Requiring only small volumes of very expensive reagents, relatively short time analysis and easy operational exhibited these

miniaturized devices have advantages over the larger counterparts. A number of miniaturized devices have been developed for sample-handling steps in integrated platforms. For example, capillary electrophoresis devices were fabricated for molecular genetics; DNA chips for high-speed DNA sequencing; microchips for polymerase chain reaction. Besides, the miniaturized devices have evolved for microelectronics with monitoring, actuating and controlling tools (microactuators, micromotors and mechanical sensors) in engineering. These current and potential applications make the microfabrication attractive and commonly used for various fields.

## 1.2 Objectives of this study

Electrochemical sensor can provide many advantages and overcome the drawback over the conventional methods for the pesticide residual detection in food. Also, with the development of the MEMS or  $\mu$ -TAS technology, the miniaturization of electrochemical sensor has made a great progress. The fabrication of electrochemical sensors in industrial level becomes possible and easy. These technologies will produce a functional chemical sensor or biosensor, which serve as the basis of for a low-cost, portable, and hand-held device for use in the field or production factory.

In my research work, two different kinds of micro electrochemical sensor for organophosphate pesticides detection were developed with the following objectives:

- 1) To design and fabricate a coulometric device for organophosphate pesticides detection
- 2) To apply the coulometric device for organophosphate pesticide detection based on different enzyme substrate and electrochemical signal.
- 3) To study the process of forming a pH sensitive electrode by plasma oxygen oxidation
- 4) To design and fabricate a micro pH-sensing device for direct determination of organophosphate pesticides.
- 5) To apply the micro pH-sensing device for direct determination of organophosphate pesticides.

Therefore, this study will focuses on clarifying the feasibility of these micro devices for the first screening detection of organophosphate pesticides to evaluate the food safety

Table 1.1 Organophosphates included in the OP Cumulative Assessment

Chemical	Decision Document	Status
Acephate	IRED	IRED completed 9/2001
Azinphos-methyl (AZM)	IRED	IRED completed 10/2001
Bensulide	IRED	IRED completed 9/2000
Cadusafos	TRED	TRED completed 9/2000
Chlorethoxyphos	TRED	TRED completed 9/2000
Chlorpyrifos	IRED	IRED completed 9/2001
Coumaphos	TRED	TRED completed 2/2000
DDVP (Dichlorvos)	IRED	IRED completed 6/2006
Diazinon	IRED	IRED completed 7/2002
Dicrotophos	IRED	IRED completed 4/2002
Dimethoate	IRED	IRED completed 6/2006
Disulfoton	IRED	IRED completed 3/2002
Ethoprop	IRED	IRED completed 9/2001 IRED addendum completed 2/2006
Fenitrothion	TRED	TRED completed 10/2000
Malathion	RED	RED completed 8/2006
Methamidophos	IRED	IRED completed 4/2002
Methidathion	IRED	IRED completed 4/2002
Methyl Parathion	IRED	IRED completed 5/2003
Naled	IRED	IRED completed 1/2002
Oxydemeton-methyl	IRED	IRED completed 8/2002
Phorate	IRED	IRED completed 3/2001
Phosalone	TRED	TRED completed 1/2001
Phosmet	IRED	IRED completed 10/2001
Phostebupirim	TRED	TRED completed 12/2000
Pirimiphos-methyl	IRED	IRED completed 6/2001
Profenofos	IRED	IRED completed 9/2000
Propetamphos	IRED	IRED completed 12/2000
Terbufos	IRED	IRED completed 9/2001
Tetrachlorvinphos	TRED	TRED completed 12/2002
Tribufos	IRED	IRED completed 12/2000
Trichlorfon	TRED	TRED completed 9/2001

Source: UNITED STATES ENVIRONMENTAL PROTECTION AGENCY  
WASHINGTON D.C., 20460.

[http://www.epa.gov/pesticides/cumulative/2006-op/op\\_ireds\\_reds\\_memo.pdf](http://www.epa.gov/pesticides/cumulative/2006-op/op_ireds_reds_memo.pdf)  
(2006-7-31)

IRED: Interim Reregistration Eligibility Decisions.



Table 1.2 Properties of Controlled-Potential Techniques

Technique	Working Electrode	Detection limit (M)
DC polarography	DME	$10^{-5}$
NP polarography	DME	$5 \times 10^{-7}$
DP polarography	DME	$10^{-8}$
DP voltammetry	Solid	$5 \times 10^{-7}$
SW polarography	DME	$10^{-8}$
AC polarography	DME	$5 \times 10^{-7}$
Chronoamperometry	Stationary	$10^{-5}$
Stripping voltammetry	HMDE, MFE	$10^{-10}$
Cyclic voltammetry	Stationary	$10^{-5}$
Adsorptive stripping voltammetry	HMDE	$10^{-10}$
Adsorptive stripping voltammetry	Solid	$10^{-9}$
Adsorptive catalytic stripping voltammetry	HMDE	$10^{-12}$

Source: Joseph Wang (2006), Analytical electrochemistry, 3<sup>rd</sup> ed. ISBN: 978-0-471-67879-3.

DP: Different pulse; SW: Square wave, NP: Normal pulse, AC: Alternating current. DME: Dropping mercury electrode, HMDE: Hanging mercury drop electrode, MFE: Mercury film electrode.

Table 1.3 Screen-printed enzymatic biosensors for pesticides detection

Immobilized enzyme	Detection
Organophosphores hydrolase	Potentiometric
Parathion hydrolase	Amperometric
Cholinesterase	Amperometric
AChE + BChE	Amperometric
AChE	Amperometric
ChO + AChE	Amperometric
BChE, ChO, HRP	Potentometric
BChE	Amperometric
ALD, Diaphorase	Amperometric
Tyrosinase	Amperometric

Source: M. Trojanowicz (2002), Determination of pesticides using electrochemical enzymatic biosensors, *Electroanalysis*, 14, 19-20.

Table 1.4 Principal methods for enzyme immobilization in biosensors

Procedure	Electrode material/immobilization agents
Adsorption	Graphite; SPE; Carbon nanotubes
Covalent binding	Pre-activated or functionalizable electrode surfaces; noble metal, graphite, SPE, Glass Glutaraldehyde, Carbodiimide/NHS
Self-assembled monolayers (SAMs) Physical entrapment	Noble metal, graphite, SPE, Glassy carbon electrode; Photopolymers; Electropolymerizable polymers; Sol-gel
Affinity	Noble metals, SPE; Silica NTA-Ni; Carbohydrates

Source: S. Andreescu et al. (2006), Twenty years research in cholinesterase biosensors: from basic research to practical application, *Biomolecular Engineering*, 23, 1-15.

Table 1.5 Examples of potentiometric transducers biosensors

Enzyme	Potentiometric Transducers	Application (analyte/detection limit)
WoAChE	pH electrode	Paraoxon (0.3ppb)
AChE	Glassy carbon electrode	Dichlorvos (0.2ppb)
BuChE	pH glass electrode	Diazinon(21ppm)
BuChE	pH-sensitive Ion selective field-effect transistors (ISFET) pH electrode pH-sensitive	MTBO Dichlorvos (0.3ppb)
AChE biotine	Light-addressable potentiometric sensor (LAPS)	Paraoxon (2.8 ppb), Bendiocarb (2.2 ppb)
AChE/ChO/HRP	Carbon electrode	Trichlofon (5.1ppb)
AChE	Fiber optic pH-sensitive electrode	Paraoxon (152ppb)
AChE/BuChE	pH-sensitive membrane (nylon, cellulose acetate)	Trichlofon (0.3ppb) Co-Ral (20ppb)

Source: S. Andreescu et al. (2006), Twenty years research in cholinesterase biosensors: from basic research to practical application, Biomolecular Engineering, 23, 1-15.

Table 1.6 Examples of bi-enzyme amperometric biosensors

Enzyme	Detection Species	Application (analyte/detection limit)	Working electrode/applied potential
AChE/ChO	H <sub>2</sub> O <sub>2</sub>	Methyl parathion (0.05 μM)	SPE with multi-wall carbon nanotubes/ +500 mV vs. Ag/AgCl (SPE)
AChE/ChO	O <sub>2</sub>	Anticholinesterase activity (binary mixtures of carbaryl. Carbofuran in concentrations 1-50 ppb)	Oxygen electrode
AChE/ChO	H <sub>2</sub> O <sub>2</sub>	Paraoxon (2.8 ppb)	Pt + 700 mV vs. Ag/AgCl
AChE/ChO	H <sub>2</sub> O <sub>2</sub>	Paraoxon (2 ppb) Aldicarb (10 ppb)	Pt + 600 mV vs. Ag/AgCl
AChE or BuChE/ChO	O <sub>2</sub>	Paraoxon, Malathion (0.3 ppb)	Clark Electrode
AChE/ChO	H <sub>2</sub> O <sub>2</sub>	Anticholinesterase/Real samples, 2ppb	SPE+700 mV vs.SCE

Source: S. Andreescu et al. (2006), Twenty years research in cholinesterase biosensors: from basic research to practical application, Biomolecular Engineering, 23, 1-15.

Table 1.7 The lowest detection limit for pesticides detection with enzymatic electrochemical biosensors.

Pesticide	Detection limit	Enzyme used
Aldicarb	2 ppb	AChE
Altrazine	4 $\mu$ M	TYR
Bendiocarb	10 nM	AChE
Carbaryl	0.5 ppb	AChE
Carbofuran	0.047 ppb	BChE
Chlorpyrifos	5 $\mu$ M	OPH
Chlorsulfuron	1 $\mu$ M	ALS
CIPC (chloroisopropyl-phenylcarbamate)	2 $\mu$ M	TYR
Co-Ral	20 ppb	AChE
Coumaphos	0.15 $\mu$ M	BChE
2,4-D	7 $\mu$ M	TYR
DDUP	0.5 ppm	BChE
DFP	1 pM	AChE
Diazinon	3 ppb	BChE
Dichlorvos	1.2 nM	AChE
Echothiophate	1 ppm	AChE
Eserine	0.37 $\mu$ M	AChE
Fenitrothion	21 ppm	BChE
Heptonophos	0.65 ppm	BChE
Hostaquick	0.3 ppm	BChE
Malathion	0.1 nM	AChE
Methomyl	0.1 ppb	AChE
Paraoxon	0.04 nM	AChE
Paraoxon methyl	0.37 $\mu$ M	AChE
Parathion	0.5 ppb	BChE
Trichlorfon	0.2 pM	BChE

Source: M. Trojanowicz (2002), Determination of pesticides using electrochemical enzymatic biosensors, *Electroanalysis*, 14, 19-20.

## REFERENCES

- [1] R. C. Gupta (2009). Handbook of Toxicology of Chemical Warfare Agents. ISBN: 978-0-12-374484-5.
- [2] [http://www.epa.gov/pesticides/cumulative/2006-op/op\\_ireds\\_recs\\_memo.pdf](http://www.epa.gov/pesticides/cumulative/2006-op/op_ireds_recs_memo.pdf) (2006-7-31).
- [3] I. Karube (2007). Handbook of Biosensors and Chemical sensors. ISBN: 978-4-924728-54-7.
- [4] J. Wang (2006), Analytical electrochemistry, 3<sup>rd</sup> ed. ISBN: 978-0-471-67879-3.
- [5] S. Andreescu, J.L Marty (2006). Twenty years research in cholinesterase biosensors: from basic research to practical application. *Biomol. Eng.*, 23, 1-15.
- [6] M. Trojanowicz (2002). Determination of pesticides using electrochemical enzymatic biosensors. *Electroanalysis*, 14, 19-20.
- [7] A. Mulchandani, W. Chen, P. Mulchandani, J. Wang, K.R. Rogers (2001). Biosensors for direct determination of organophosphate pesticides. *Biosens. Bioelectron.*, 16, 225– 230.
- [8] C. Tran-Minh, P.C. Pandey and S. Kumaran (1990). Studies on acetylcholine sensor and its analytical application based on the inhibition of cholinesterase. *Biosensors Bioelectron.*, 5, 461-471.
- [9] M. Nygamsi Hendji, N. Jaffrezic-Renault, C. Martelet, P. Clechet, A. A. Shulga, V. I. Strikha, L. I. Netchipruk, A. P. Soldatkin, W. B. Wlodarski (1993). Sensitive Detection of Pesticides Using a Differential ISFET-Based System with Immobilized Cholinesterases. *Anal. Chim. Acta.*, 28(1), 3–11.

- [10] P. Skládal, M. Mascini (1992). Sensitive detection of pesticides using amperometric sensors based on cobalt phthalocyanine-modified composite electrodes and immobilized cholinesterase. *Biosens. Bioelectron.*, 7, 335-43.
- [11] S. Kumaran, C. Tran-Minh (1992). Insecticide determination with enzyme electrodes using different enzyme immobilization techniques. *Electroanalysis*, 4, 949-954.
- [12] S. Kumaran, M. Morita (1995). Application of a cholinesterase biosensor to screen for organophosphorus pesticides extracted from soil. *Talanta*, 42, 649–655.
- [13] G. A. Evtugyn, E. P. Rizaeva, E. E. Stoikova, V. Z. Latipova, H. C. Budnikov (1997). The application of cholinesterase potentiometric biosensor for preliminary screening of the toxicity of waste waters. *Electroanalysis*, 9, 1124–1128.
- [14] L. Campanella, R. Cocco, M.P. Sammartino, M. Tomassetti (1992). A new enzyme inhibition sensor for organophosphorous pesticide analysis. *The Science of the Total Environment*, 123/124, 1-16.



## CHAPTER 2

### **Microfluidic Device for Coulometric Detection of Organophosphate Pesticides based on Acetylcholinesterase Inhibition**

#### **2.1 Introduction**

Organophosphate pesticides (OPs) are highly toxic because they inactivate acetylcholinesterase (AChE), an enzyme required for nerve function [1]. They form covalent bonds to serine residues that are located in the active site of AChE, impairing the enzyme function. Subsequent build-up of acetylcholine blocks cholinergic nerve impulses, leading to paralysis, suffocation, and ultimately to death [2].

Conventional methods including high performance liquid chromatography, gas chromatography coupled chromatographic-spectrometric were used in analytical lab but they suffer time-consuming, because of the extensive preparation steps required, including extraction and purification, making them unsuitable for in situ or real-time detection. Besides, they are very expensive and require highly qualified personnel [1].

To solve this problem, biosensing techniques based on the cholinesterase enzyme (ChEs) can be rapid, simple and reliable alternative to the classical methods [2-5]. Various electrochemical biosensors was created and developed [6]. Among them, amperometric transducer coupled with AChE inhibition was selected to be the principal choice due to its high sensitivity [7-12]. The biosensors based on this principle offered many advantages such as high sensitivity, rapid response, and good stability. The method of immobilization of enzymes onto an electrode has been improved, and the problem of the regeneration of the biosensor caused by irreversible inhibition of AChE by OPs was overcome by the application of bio-labelled magnetic beads [5]. With the progress of the development of the micro-total system ( $\mu$ TAS) or Lab-on-a-Chip technologies, microfluidics have been proposed as a promising technique [13-19]. The plug-based microfluidics can reduce the

volume of very expensive reagents significantly and facilitate handling of many solutions in a limited space. In detecting analytes in the plugs, amperometry is often used. However, sensitive amperometric detection becomes more difficult with decreasing sample and reagent volumes. In this respect, coulometry is more advantageous. The final output signal in coulometry method is obtained in the form of charge, which is the integral of the current, signifying the analyte is obtained not as concentration but as the amount of analyte that reacts on the detecting electrode. In our previous study, we have successfully investigated the applicability of coulometry on the detection of L-glutamate and hydrogen peroxide ( $H_2O_2$ ) in a plug placed in a flow channel [20].

OPs based on two-step bienzyme reactions of AChE and choline oxidase and coulometric detection of one of the final reaction products,  $H_2O_2$  were firstly introduced. The enzyme plug and substrate plug were formed in the flow channel by rhombuses structure and the final product was determined at the electrode area. In processing plugs of aqueous solutions, the interior of the flow channels must be sufficiently hydrophobic. Otherwise, plugs collapse while they are moved. Here, a problem is surface state changes by the adsorption of proteins. The influence of using the two enzymes was no negligible and residue of enzymes on the wall of the channel often happened. In addition, the use of the two enzymes increases cost [21]. To solve the problems, a coulometric device used mono-enzyme system based on the detection of TCh was fabricated.

Thiocholine (TCh) is one of the enzyme reaction products of AChE with acetylthiocholine (ATCh) as an enzyme substrate. Therefore, TCh has been used as an indicator to measure the activity of AChE for the detection of OPs, carbamic pesticide, or nerve agents [22,23]. Currently, spectrophotometric detection using Ellman's method is often carried out to measure TCh, which is based on the detection of the produced TCh [24]. The detection is based on a reaction that uses TCh and 5,5'-dithiobis-2-nitrobenzoic

acid (DTNB) to produce 2-nitro-5-thiobenzoic acid (TNB) with yellow color [24]. Compared with the spectrophotometric detection, electrochemical methods have many advantages including rapid response, relative high sensitivity, and good stability when incorporated in miniaturized devices [24-27]. Moreover, the whole measurement is simpler and can be carried out by no skilled personnel.

In this chapter, I focused my attention on the design and fabricate of electrochemical device. One is the Coulometric device based on bienzymes system and the other is based on mono-enzyme system. The microfabrication technique was used and the microfabrication procedure of the microdevice was introduced and described. The miniaturized device required only small volumes of very expensive reagents, relatively short time analysis and easy operational in integrated platforms.

## **2.2 Experimental section**

### **2.2.1 Reagents and materials**

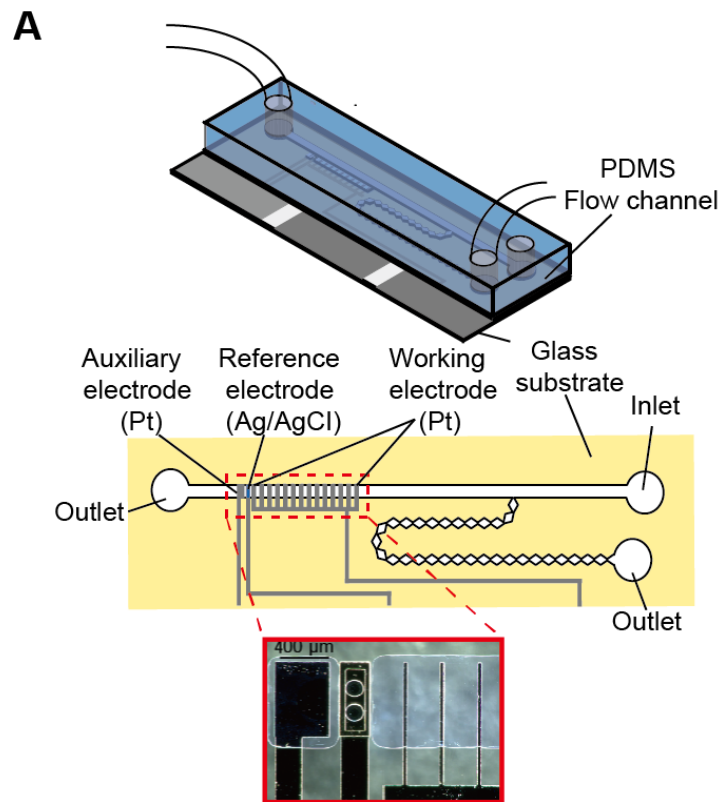
The reagents and materials used for the fabrication and characterization of the device were obtained from the following commercial sources: glass wafers (#7740, 3-in. diameter, 500- $\mu$ m thickness) from Corning Japan (Tokyo, Japan); thick-film photoresist, SU-8 25, from Microchem (Newton, MA, USA); and prepolymer solution of polydimethylsiloxane (PDMS), KE-1300T, from Shin-Estu Chemical (Tokyo, Japan). AChE (EC 3.1.1.7, from *Electrophorus electricus*, 827 units/mg), ChOx (EC 1.1.3.17, from *Alcaligenes* spp., 13 units/mg), and acetylcholine chloride were purchased from Sigma-Aldrich (St. Louis, USA). A 50 mM phosphate buffer solution (PBS) was used to dissolve the AChE and ChOx. Hydrogen peroxide (30%) was purchased from Wako Pure Chemical Industries (Osaka, Japan). Commercial OP formulations (malathion, acephate, MEP, diazinon) were purchased from Sumitomo Chemical Garden Products\_(Tsukuba, Japan). Organic solvents

were purchased from Wako (Osaka, Japan). All OP solutions were prepared with a 0.1 M KCl solution. For analysis on the device, a solution containing ACh (Solution A) and a solution containing an OP and the two enzymes (Solution B) were prepared. All reagents were of analytical grade and all experiments were performed at room temperature.

### **2.2.2 Device fabrication**

The microdevice consisted of a glass substrate with a three-electrode system to measure charge and a PDMS substrate with a flow channel structure (Fig. 2.1). The fabrication process was described in details. The three-electrode system consisted of a platinum working electrode, an Ag/AgCl reference electrode, and a platinum auxiliary electrode. The working electrode consisted of a microelectrode array (40 thin strips of  $600\ \mu\text{m} \times 400\ \mu\text{m}$ ) with a  $130\text{-}\mu\text{m}$  inter-electrode distance (edge to edge). The microelectrode array was effective to achieve highly sensitive detection by reducing the background [25]. Two pinholes ( $30\ \mu\text{m}$  in diameter) were formed on the silver layer of the reference electrode. AgCl was grown from the pinholes into the silver layer by applying a current of 50 nA for 20 min in a 0.1 M KCl solution. This structure realized excellent durability for reliable coulometric measurement [29]. The flow channel structure including the main and auxiliary flow channels was formed with PDMS by replica molding using a template formed with the thick-film photoresist (SU-8). A T-junction formed with the main and auxiliary flow channels was used to form and manipulate solution plugs. The auxiliary flow channel consisted of an array of rhombuses. The shape of the rhombuses was designed so that solutions occupy each rhombus as a unit depending on the applied pressure by taking advantages of changes in surface tension in the structure [26]. A T-junction was formed in the PDMS flow channel structure to process solutions (Fig. 2.2). Through holes were formed at the end of the main and auxiliary flow channels by

punching and silicone tubes (inner diameter: 500 $\mu$ m) were connected there to introduce solutions and apply pressure.



**B**

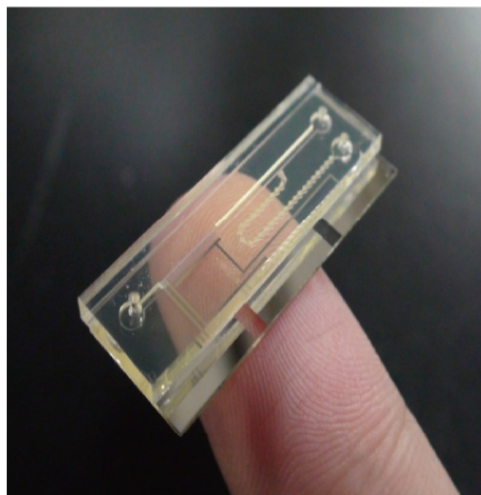


Fig. 2.1 The fabricated device. A: Exploded view of the device.

B: The device on a finger. Planar dimensions are 30 mm  $\times$  11 mm.

The flow channel structure, consisting of a main flow channel and an auxiliary flow channel connected at a T-junction, was formed with PDMS by replica molding using a template formed with the thick-film photoresist (SU-8). In the auxiliary flow channel, an array of rhombus structures was formed for precise measurement of solution volumes by surface tension [30]. To collect diffusing electrochemically active products on the working electrode more efficiently, the height of the sensing region in the flow channel was constricted to 60  $\mu\text{m}$ .

The detailed fabrication procedure is described as below based on MEMS technique and standard photolithography.

### **(1) Fabrication of the on chip electrode (Fig. 2.2)**

#### Cleaning of glass substrate

First, prepare the washing solution (25%  $\text{NH}_3 \cdot \text{H}_2\text{O}$ : 30%  $\text{H}_2\text{O}_2$ : deionized water = 1 : 1 : 4) and boil it. Then, immerse the glass substrate into the boiled washing solution and boiled deionized water in sequence for 5 min, respectively. After that, wait the glass substrate dry by itself.

#### Formation of Pt/Cr lift-off pattern for coulometric device

Spin coat the positive photoresist (S1818G) was spin coated (500 rpm, 5 s  $\rightarrow$  2000 rpm, 10 s) onto the surface of the clean glass substrate and baked in the dry oven for 30 min (80  $^\circ\text{C}$ ). Then, form the Pr/Cr lift-off pattern with the designed mask by being exposed under ultra violet emitted by mask aligner for 60 s. After that, immerse the glass substrate into the 30  $^\circ\text{C}$  toluene for 30 s and bake it in the 80  $^\circ\text{C}$  dry oven for 15 min. Finally, develop the glass substrate in the positive photoresist developer for 1 min, rinse it with deionized water and dry it with  $\text{N}_2$  gas;

#### Sputtering of Pt/Cr for coulometric device

For coulometric device, sputter the Cr layer (5 min) and Pt layer (15 min  $\times$  2) on the glass substrate by sputtering machine. The output power was maintained at 100 W throughout the procedure.

#### Lift-off of Pt/Cr layer for coulometric device

For coulometric device, immerse the glass substrate that already sputtered metal layer in the acetone for at least 1 h. Then, peel the Pt/Cr layer where does not cover the electrode region. At last, wash the glass substrate again with acetone and dry it with N<sub>2</sub> gas.

#### Formation of Ag lift-off pattern for both devices

Spin coat the positive photoresist (S1818G) again (500 rpm, 5 s  $\rightarrow$  2000 rpm, 10 s) and bake the glass substrate in the 80 °C dry oven for 30 min. Then, form the Ag lift-off pattern on the glass substrate with the designed mask by being exposed under ultra violet emitted by mask aligner for 1 min. After that, immerse the glass substrate in the 30 °C toluene for 30 s and bake it in the 80 °C dry oven for 15 min. Finally, develop the glass substrate in the positive photoresist developer for 1 min, rinse it with deionized water and dry it with N<sub>2</sub> gas.

#### Sputtering of Ag for the device

For coulometric device, sputter the Ag layer on the glass substrate by sputtering machine twice, each time for 15min. The output power was maintained at 100 W during the sputtering process.



### Lift-off of Ag layer for the device

Immerse the sputtered glass substrate in the acetone for at least 1 h. Then, peel the Ag layer where does not cover the electrode region from the glass substrate. Finally, wash the glass substrate again with acetone and dry it with N<sub>2</sub> gas.

### Formation of insulating layer

Spin coat the insulating layer (polyimide layer), polyimide (500 rpm, 10 s → slope, 5 s → 4000 rpm, 30 s) on the Pt/Cr/Ag patterned glass substrate and bake the glass substrate in the 80 °C dry oven for 30 min.

### Formation of positive photoresist layer

Spin coat positive photoresist (S1818G) on the glass substrate (500 rpm, 5 s → 2000 rpm, 15 s) and bake it in the 80 °C dry oven for 30 min.

### Formation of insulating layer pattern

Form the insulating layer, polyimide pattern mask were used under the ultra violet emitted for exposure by mask aligner for 1 min. Then, immerse the glass substrate in the positive photoresist developer for 1 min. Finally, immerse the glass substrate in the ethanol and strip off the positive photoresist layer.

### Cure of insulating layer

Put the glass substrate on the hot plate and cover it (150 °C, 15 min → 200 °C, 15 min → 280 °C, 30 min) for curing the insulating layer, polyimide.

### Dicing

Spin coat positive photoresist (S1818G) (500 rpm, 15 s → 2000 rpm, 15 s) on the glass substrate for protecting the on chip electrode during the dicing and bake the glass substrate in the 80 °C dry oven for 30 min. Then, immobilize the glass substrate on the immobilization sheet. Finally, cut the glass substrate into devices one by one and rinse the protection layer with acetone and deionized water. The size of one chip was 30 mm × 15 mm for coulometric device

### Formation of Ag/AgCl layer for the device (Fig. 2.3)

Two pinholes of 30 μm in diameter for coulometric device and five pinholes of 50μm in diameter were formed on the silver layer of the reference electrode, where AgCl was grown by applying a current of 50 nA for 20 min in a 0.1 M KCl solution.

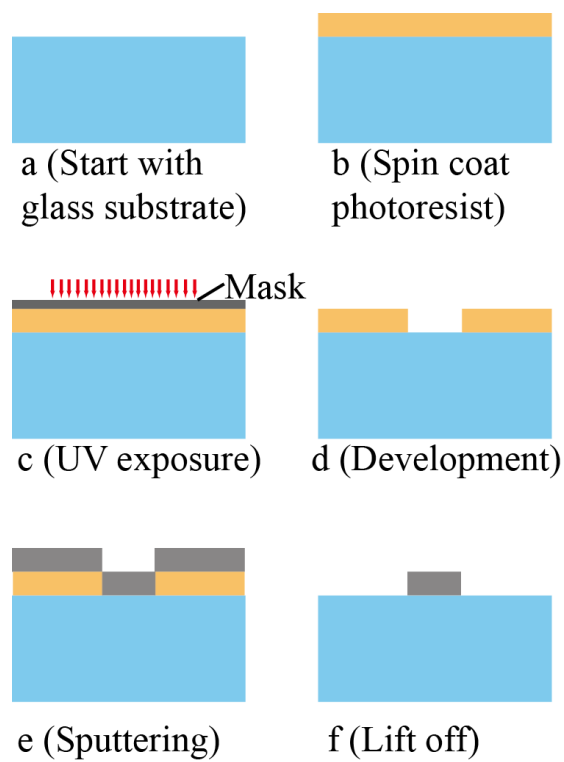


Fig. 2.2 Schematic illustration of the fabrication of on chip electrode for coulometric device.

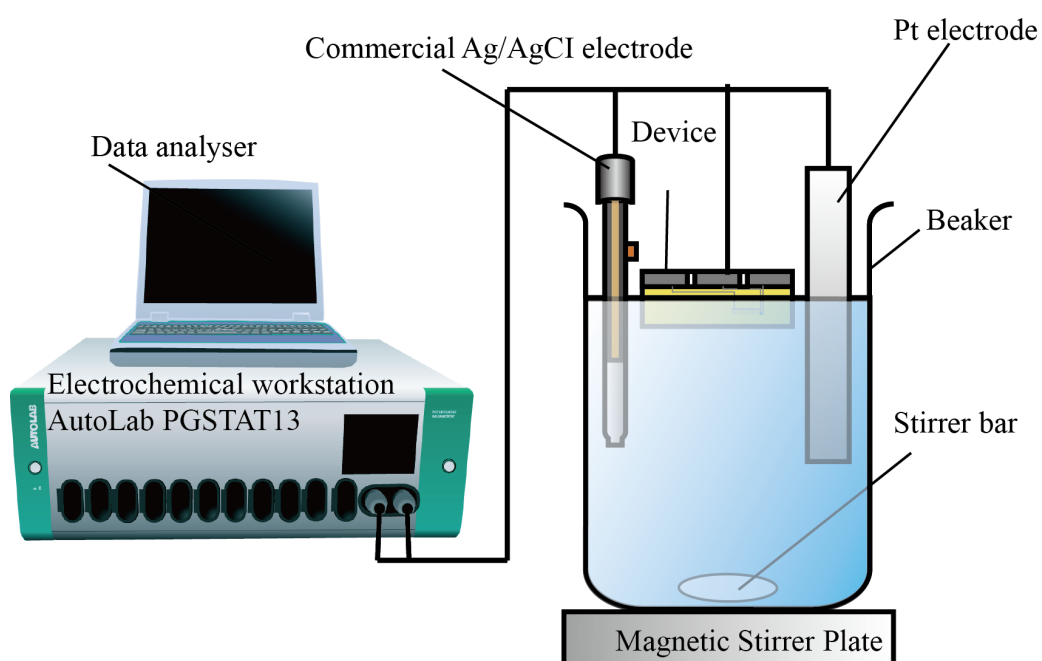


Fig. 2.3 Schematic illustration formation of Ag/AgCl layer on the device.

## **(2) Fabrication of PDMS substrate**

### Cleaning glass substrate

First, prepare and boil the washing solution (25%  $\text{NH}_3 \cdot \text{H}_2\text{O}$  : 30%  $\text{H}_2\text{O}_2$  : deionized

water = 1 : 1 : 4). Then, immerse the glass substrate into the boiled washing solution and boiled deionized water in sequence for 5 min, respectively. After drying, put the substrate in the oxygen plasma chamber for plasma cleaning for 1 min. The output power was set at 100 W during the plasma cleaning.

#### Formation of SU-8 pattern for lower part

Spin coat SU-8 (500 rpm, 5 s → slope, 10 s → 800 rpm, 15 s) onto the glass substrate and pre-bake the glass substrate on the hot plate at 65 °C for 5 min and 95 °C for 25 min, respectively. Then, form the SU-8 pattern (lower part) by using the mask under the UV exposure for 180s. After exposure, bake the glass substrate on the hot plate at 65 °C for 10 min.

#### Developing of SU-8 (lower part)

Develop and rinse SU-8 in the SU-8 developer solution. Besides, wash the glass substrate with 2-propanol to preventing from contamination. Then, dry the glass substrate with N<sub>2</sub> gas.

#### Cleaning of glass substrate

Clean the surface of lower part SU-8 patterned glass substrate with oxygen plasma for 3 min. The output power was maintained at 100 W.

#### Formation of SU-8 pattern for higher part

Spin coat SU-8 (500 rpm, 5 s → 2000 rpm, 15 s) onto the glass substrate. Additionally, put a more than 3 g SU-8 on the glass substrate after spin coat. Then, put the glass substrate on the hot plate with a cover at 65 °C and 95 °C for 10 min and 8 h, respectively.

After that, form the mask for higher part SU-8 pattern was used for exposure for 480 s. Finally, bake the glass substrate again on the hot plate at 65 °C for 20 min.

#### Developing of SU-8 (higher part)

Develop and rinse SU-8 in the SU-8 developer. Clean the glass substrate in 2-propanol to get rid of contamination. Then, dry with N<sub>2</sub> gas.

As far as, the SU-8 template was finished. The PDMS substrate was carried out based on the SU-8 template.

#### Preparation of PDMS substrate for the device

Mix the precursor solution of PDMS (KE-1300T) and curing solution (CAT-1300) with a mass ratio of 10 : 1. Then, pour the mixture on the surface of the SU-8 template uniformly and vacuumed it to get rid of foam in a vacuum pump. After that, cure the PDMS in the 80 °C dry oven for 30 min and strip off it from SU-8 template. Finally, cut the PDMS into pieces one by one according to the design dimensions.

### **2.2.3 On-chip processing of liquid plugs**

Fig. 2.4 shows the procedure used to process plugs at the T-junction. Arbitrary volumes of solutions A and B were first introduced from the inlet into the main flow channel. An appropriate positive or negative pressure was applied to the end of the main and auxiliary flow channels to adjust the position of the solutions and to measure the volumes required. A volume that corresponded to four rhombuses was equal to the volume of the sensing region (300 nL). Two rhombuses (150 nL) of the auxiliary flow channel were used to form each plug (i.e., 1:1 volume ratio). To begin the analysis, the solutions were ejected from the auxiliary flow channel and merged in the main channel, aided by the T-junction [31].

To mix the solution components in the new plug, it was moved around, and then the plug of the mixture was transported to the sensing region for coulometry. After each measurement, PBS was injected into the flow channel to wash the sensing region.

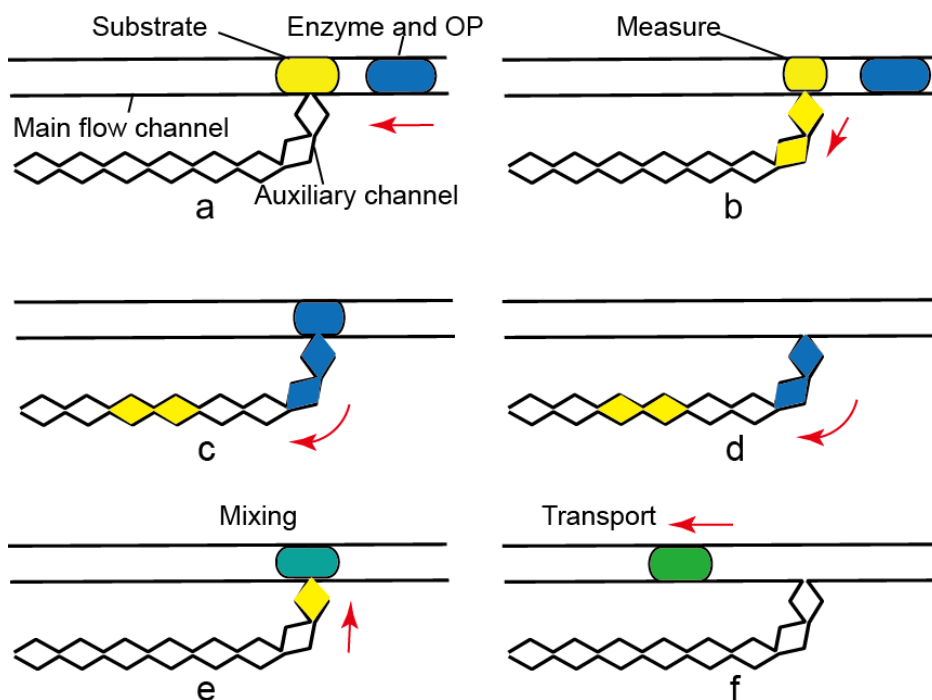


Fig.2.4 Steps in processing plugs of solutions. (a) A substrate solution and a solution containing enzymes and an OP were introduced into the main flow channel. (b-d) The volume of each plug was measured using the auxiliary flow channel and the parts of the plugs in the main flow channel were discarded. (e) The two plug solutions were merged in the main flow channel. (f) The new plug was transported to the sensing region and the components were mixed.

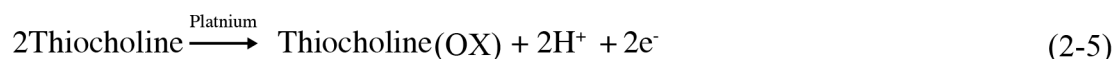
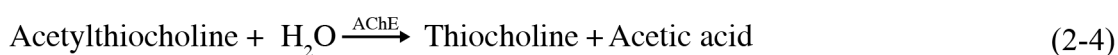
## 2.2.4 Principles underlying coulometric detection of OPs

For coulometric detection of organophosphate pesticides based on bienzyme system, the enzymatic and electrochemical reactions used for the detection of OPs are described as follows:



First, choline (Ch) is produced from the substrate acetylcholine (ACh) and then  $\text{H}_2\text{O}_2$  is produced by the enzymatic reaction catalyzed by ChOx. The final electrochemical active product,  $\text{H}_2\text{O}_2$ , is oxidized electrochemically, and finally the charge generated is recorded. In the presence of OPs, the inhibitor OPs inhibits the activity of AChE. Therefore, the decrement in the charge can act as an indicator of AChE inhibition. In this study, commercial formulations of malathion, acephate, diazinon, and MEP were employed as model OPs.

For coulometric detection of organophosphate pesticides based on mono-enzyme system, the enzymatic and electrochemical reactions used for the detection of OP are as follows:



OPs are well-known inhibitors of AChE. In this part, ATCh was used as the substrate of AChE to measure a change in the AChE activity before and after the incubation with the OP. The degree of inhibition was calculated using the following equation:

$$\text{Inhibition (\%)} = \frac{q_1 - q_2}{q_1 - q_0} \times 100 \quad (2-6)$$



where  $q_0$  is the background charge in the absence of the OP and the enzyme,  $q_1$  is the charge when the enzyme is not inhibited, and  $q_2$  is the charge when the enzyme is inhibited by the OP. The reduced activity of AChE leads to the decrease in the production of TCh, which then results in the decrease in current or charge generated on the working electrode. Therefore, the decrease in the measured charge can be related to the inhibitory effect of the OP or its concentration. In this study, malathion was used as a model OP.

### **2.2.5 Measurement procedure**

For coulometric detection of organophosphate pesticides based on bienzyme system, while conducting the coulometric analysis, the substrate ACh solution was first introduced into the main flow channel and the volume was measured by the auxiliary flow channel, and the signal produced by the uninhibited enzymatic reactions was registered. After flushing the solutions and rinsing the flow channel with PBS, an OP standard solution containing the bienzyme solutions was loaded into the flow channel, and the change in signal originating from the inhibition of AChE was recorded. The coulometric measurement was performed using an electrochemical workstation (Autolab PGSTAT13, Eco Chemie, Utrecht, The Netherlands) connected to a personal computer. Measurements were performed in triplicate, with the exception of the experiments, which were performed once. The potential applied to the working electrode was + 0.7 V.

For coulometric detection of organophosphate pesticides based on Mono-enzyme system, a solution containing ATCh and a solution containing malathion and the enzyme were introduced into the flow channel and were processed in the form of liquid plugs. The volumes of the solutions were measured using the rhombus structure in the auxiliary flow channel and the solutions were mixed by an operation using the T-junction. In measuring the volume of a solution, a solution plug was introduced into the auxiliary flow channel by

applying a negative pressure to the flow channel. The rhombus structure was designed so that the solution moved spontaneously once it passed the widest portion and stopped at the narrowest portion by capillary action. Two rhombuses (150 nL) were used to form each plug and a volume that corresponded to four rhombuses was equal to the volume of the sensing region (300 nL) [10]. Coulometry was conducted using an electrochemical workstation (Autolab PGSTAT13, Eco Chemie, Utrecht, The Netherlands) connected to a lap top computer. The potential applied to the working electrode was + 0.65 V with respect to the on-chip Ag/AgCl reference electrode [25]. After each measurement, the electrodes and the flow channel were washed with PBS.

For the coulometry, TCh was produced by the enzymatic reaction and was accumulated for 30 min in the plug of the merged solutions. The coulometry started by introducing the substrate (ATCh) and enzyme (AChE) solutions into the flow channel structure and merging the plugs of the solutions. The signal produced accompanying the enzymatic reaction ( $q_1$ ) was recorded. After flushing all used solutions in the flow channel structures and washing them with PBS, a malathion standard solution containing AChE was introduced into the flow channel along with the substrate solution. After merging the plugs of the solutions, the change generated by the inhibited AChE was measured ( $q_2$ ). The concentration of ATCh was fixed at 2 mM.

## **2.3 Results and Discussion**

### **2.3.1. Coulometric detection of $H_2O_2$ and the stability of the microfabricated device**

To characterize the performance of the device, detection of the final product,  $H_2O_2$ , was first verified. Fig. 2.5 shows the relationship between the output charge and the  $H_2O_2$  concentration. A strongly linear relationship was observed for concentrations ranging from

10  $\mu\text{M}$  to 1 mM ( $R^2 = 0.997$ ). Scattering of the output charge was small ( $\text{RSD} = 2.8\%$ ) in 20 consecutive measurements shown in Fig. 2.6, indicating that the device is acceptably stable during consecutive measurements.

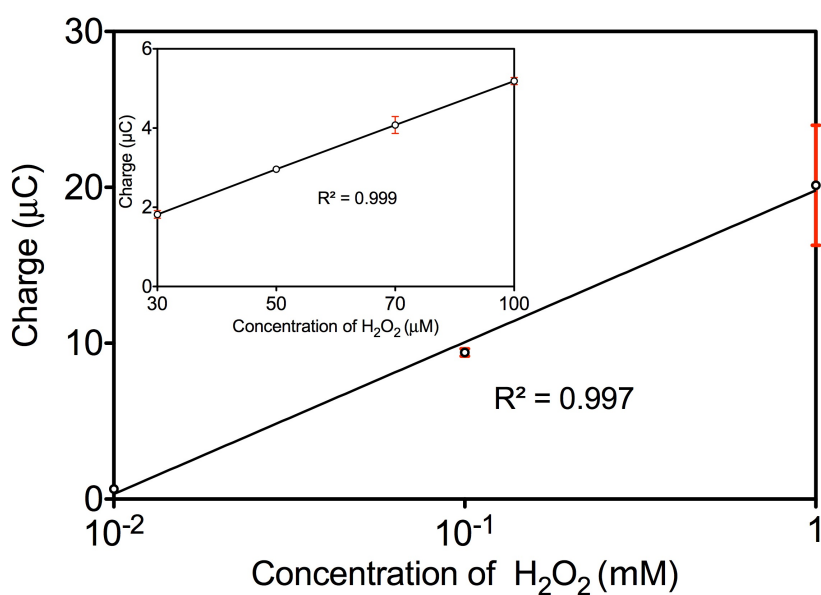


Fig. 2.5 Dependence of charges on the concentration of  $\text{H}_2\text{O}_2$ . The inset shows the plot at lower  $\text{H}_2\text{O}_2$  concentrations. Each data point represents the average of three measurements; averages and standard deviations are shown.

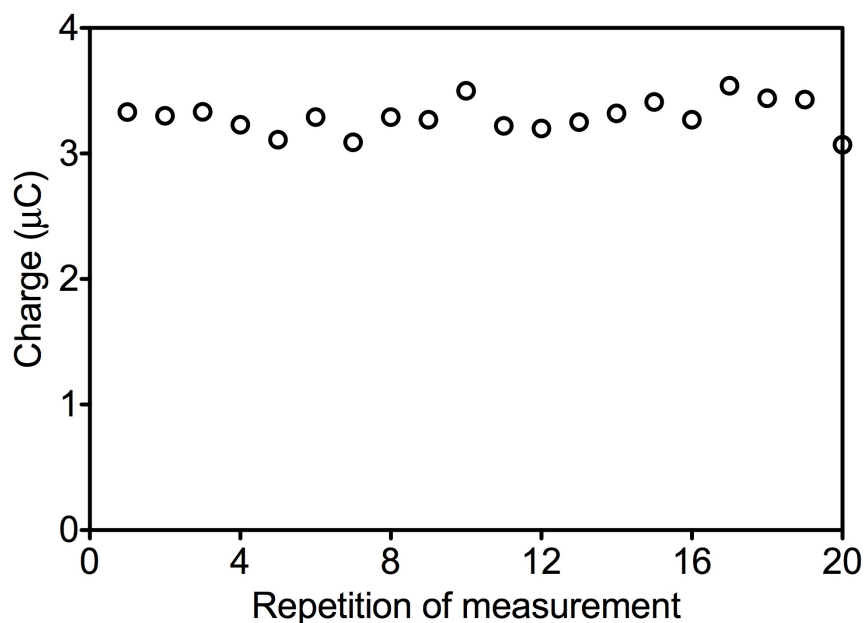


Fig. 2.6 Reproducibility of the output charge obtained with 100 mM H<sub>2</sub>O<sub>2</sub>.

### 2.3.2 Detection of OPs by AChE inhibition

Determination of the OP concentration is based on measurement of the change in AChE activity. Michaelis-Menten kinetics suggests that enzyme activity depends on the concentration of the substrate; it becomes saturated at the concentrations sufficiently higher than the Michaelis constant ( $K_m$ ). Thus, the concentration of substrates must be sufficiently high to minimize changes in activity caused by changes in substrate concentration. In practice, the concentration is set at a value that is approximately 10–20 times the  $K_m$  value (100  $\mu$ M for ACh) [29]. Hence, the final concentration of ACh was set at 1 mM. Fig. 2.7 shows that the inhibition of AChE was evident when 100  $\mu$ M malathion and the two enzymes were incubated for 7 min. The generated charge tended to saturate

after 7 min, which indicated that the binding sites between AChE and OPs had been saturated and reached equilibrium. The extent of inhibition was calculated using the following equation (2-6), where  $q_0$  is the background charge in the absence of OPs and enzymes,  $q_1$  is the charge when the enzyme is uninhibited, and  $q_2$  is the charge when the enzyme is inhibited by OP. For detection of OPs, the curves shown in Fig. 2.8 demonstrate that the linear range was  $10^{-10}$ – $10^{-2}$  M for malathion ( $R^2 = 0.982$ ), acephate ( $R^2 = 0.956$ ), and MEP ( $R^2 = 0.963$ ). For diazinon, the linear range was  $10^{-12}$ – $10^{-6}$  M ( $R^2 = 0.935$ ). The detection of limit for malathion was 33 nM ( $3\sigma$ ). For acephate, MEP, and diazinon, the detection limit was 90 nM ( $3\sigma$ ). As shown in Fig. 2.7, a clear linear relationship was observed between the AChE inhibition rate and the logarithm of the concentration of the OP formulations, demonstrating that the microfabricated OP detection device can be used for precise detection of OPs.

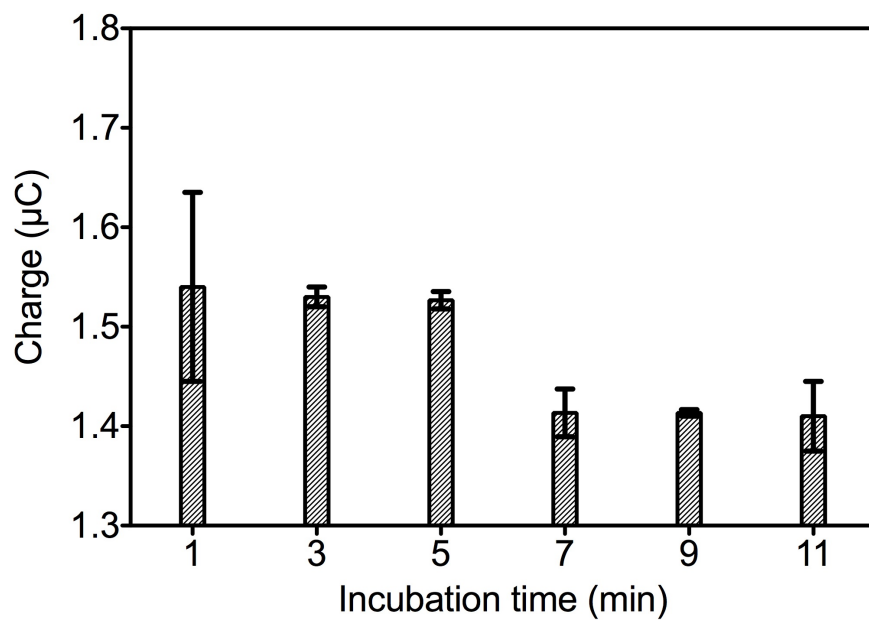


Fig. 2.7 Charge measured accompanying the enzymatic reactions in the presence of 100  $\mu\text{M}$  OP after pre-incubation for various time. Each data point represents the average of three measurements; averages and standard deviations are shown.

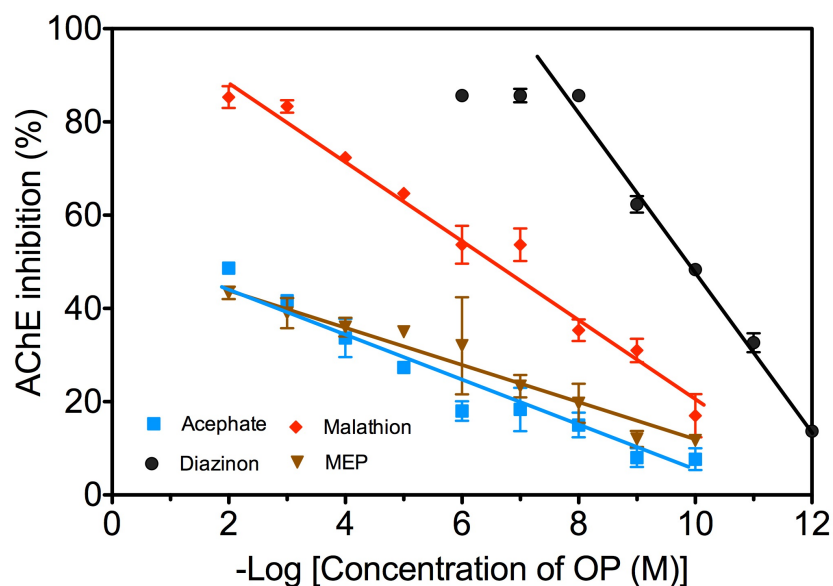


Fig. 2.8 Calibration plots obtained for commercial formulations of OPs. Each data point represents the average of three measurements; averages and standard deviations are shown.

### 2.3.3 Influence of organic solvents

Considering that commercial formulations of OPs contain some organic solvents, including polar and non-polar organic solvents, such as 2-propanol, ethanol, chloroform, and xylene, therefore, we also investigated the effect of organic solvents on the activity of AChE, using both pure organic solvents and mixtures of water and polar organic solvents. The percent inhibition was calculated using the equation given above, where the charge obtained at 8 min after AChE was incubated in organic solvent was used for  $q_2$ . Measuring AChE activity in different pure organic solvents revealed that AChE activity was markedly decreased (Fig. 2.9). However, AChE activity was higher in mixtures of water and 2-propanol than in pure 2-propanol, when the percentage of 2-propanol was 10–40%. The

same effect was observed using a water-ethanol mixture, but no inhibition was observed with 5% ethanol. Thus, organic solvents interfere with the results when their concentration is of the order of several tens of a percent, which are several orders of magnitude higher than the influential concentration of OPs. Therefore, organic solvents exert a negligible influence on the analysis.

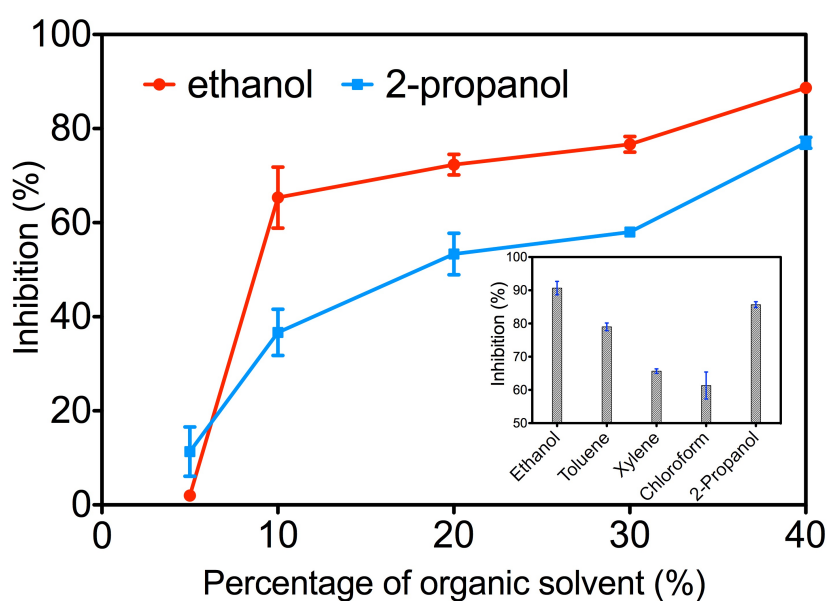


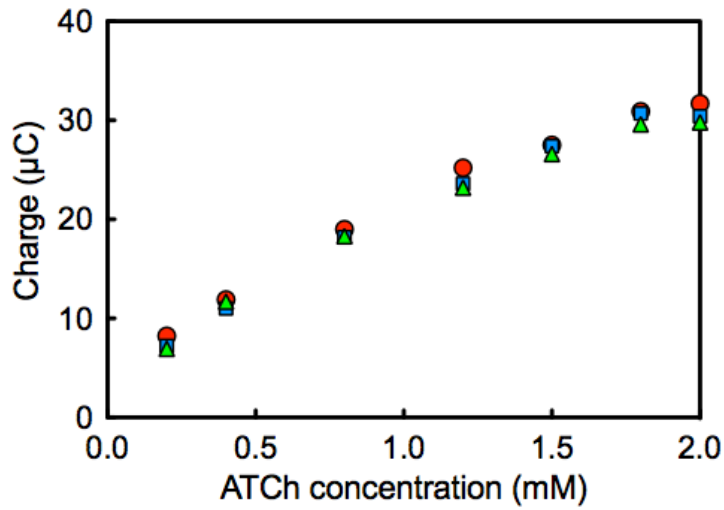
Fig. 2.9 Inhibition of AChE after 8-min incubation in 5–40% polar organic solvents. The inset shows data obtained using pure organic solvents. Each data point represents the average of three measurements; averages and standard deviations are shown.



### 2.3.4 Coulometric detection of organophosphate pesticides based on Mono-enzyme system

As a first step, the response of the device to ATCh was checked without the enzyme and malathion. Fig. 2.10 shows the calibration plot for ATCh determination obtained by successive additions of the substrate. A linear relationship was observed in a concentration range between 0.4 and 1.2 mM ( $R^2 = 0.991$ ) with a sensitivity of 4.88 mC/M. The curve gradually saturated with the increase in the ATCh concentration. The apparent Michaelis-Menten constant,  $K_m^{app}$ , for ATCh determined by electrochemical Eadie-Hofstee form of the Michaelis-Menten equation was 0.66 mM [27]. Relative standard deviation (RSD) was within 3.2 % for values obtained in triplicate measurements, demonstrating reproducible measurements using the device.

A



B

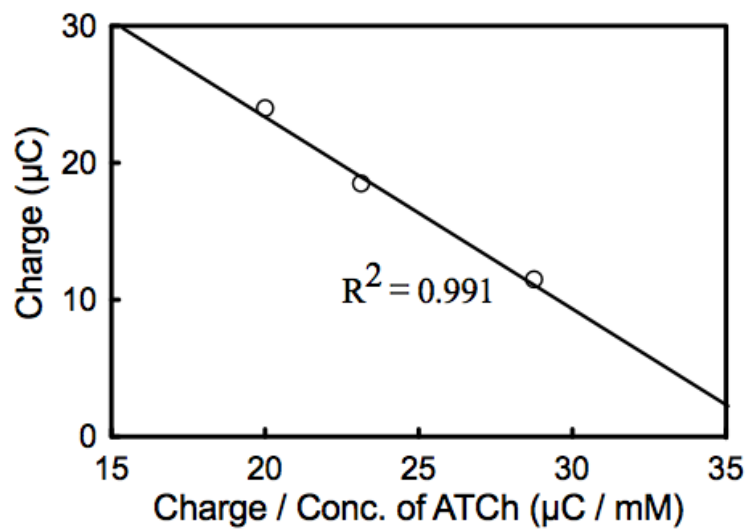


Fig. 2.10 The influence of the substrate (ATCh) on final charge.

A: Dependence of the generated charge on the concentration of ATCh. The symbols correspond to three measurements.

B: Calibration plot for the device obtained by successive additions of the substrate.

### 2.3.5 Temperature dependence

In order to choose the best condition for ATCh detection, the influence of temperature on the enzyme activity was investigated. Responses were measured at 25°C, 37°C, and 50°C. The room temperature set at 25 °C for the measurement at 25 °C. For experiments at 37°C and 50°C, the chips were placed on a hot plate, respectively. As shown in Table 2.1, the enzyme activity decreased monotonically with the increase in temperature, and the maximum response was obtained at 25°C among the three temperatures. Although deactivation of the enzyme is anticipated at higher temperatures, the measured charge was substantial even at 50°C. Although a higher activity may be observed at temperatures between 25 and 37°C, formation of air bubbles dissolved in the main flow channel became more significant when the temperature was elevated. No such troubles were experienced at 25°C. Therefore, all the measurements were carried out at 25°C.

Table 2.1 Charge measured accompanying the enzymatic reactions at different temperature. ATCh concentration: 2 mM. Each point in the graph represents the average of three measurements. Standard deviations are also shown.

Temperature (°C)	Charge (μC)
25	7.63 ± 0.31
37	7.05 ± 0.12
50	3.50 ± 0.66

### 2.3.6 Detection of malathion using the device

Determination of malathion was carried out based on the enzymatic and electrochemical reactions mentioned earlier. The inhibition of AChE by OPs is irreversible. Fig. 2.11 shows calibration plots that represent the inhibition of AChE activity as a function of malathion concentration. The graph displayed linearity ( $R^2 = 0.951$ ) in a concentration range between  $10^{-6}$  M and  $10^{-3}$  M. The lower limit of detection was 412 nM, which is comparable with that of previous reports [23-25]. Gogol et al. and Arduini et al. designed a screen-printed electrodes coated biosensors with  $3.5 \times 10^{-7}$  M for trichlorfon,  $1.5 \times 10^{-7}$  M for coumaphos [23] and  $5 \times 10^{-7}$  M detection limit [24], respectively; Liu et al. used a carbon nanotube modified glassy carbon electrode for TCh detection with a detection limit  $3 \times 10^{-7}$  M for TCh [25]. The lower limit of detection we obtained was 412 nM, which is comparable with those of previous reports based on the same TCh detection. The maximum residue levels (MRLs) represents the upper legal limit of the concentration of pesticide residues in food. The Table 2.2 summarizes the MRLs of malathion for various foods in U.S.A, Canada, and Mexico [28]. The maximum residue level (MRL), which represents the upper legal limit of the concentration of pesticide residues in food, for malathion is 0.01 - 8 ppm (30.2 nM - 24.2  $\mu$ M) according to the Japan Food Chemical Research Foundation. Therefore, the lower limit of detection achieved using our device is sufficient to detect malathion of the concentrations of this order. To lower the detection limit further, a longer incubation time and use of other enzymes with a smaller  $K_m$  value will be effective to improve the detection limit [23,29]. In this experiment, the incubation time for the mixture of malathion and AChE was 7 min. Therefore, there is still room to improve the performance if the requirement for the length of the incubation time is not so severe. Nevertheless, the device can reduce the consumption of very expensive reagents and can simplify the processing of solutions. In this sense, the device can be useful in

realizing portable user-friendly instruments for on-site analyses of OPs.

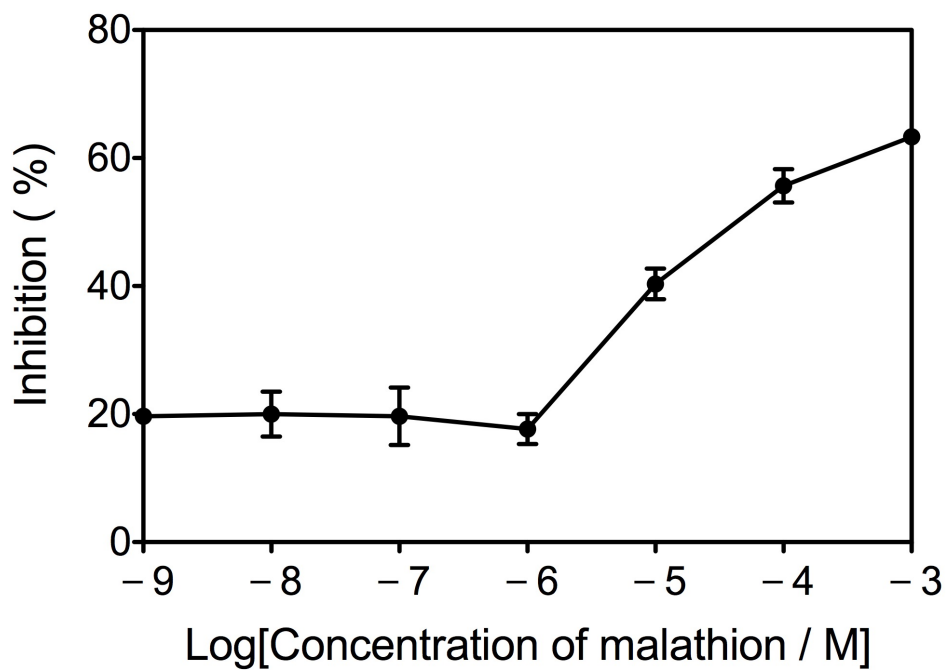


Fig. 2.11 Dependence of AChE inhibition on the concentration of malathion.

Each point in the graph represents the average and standard deviations of three measurements.

Table 2. 2 Summary of Current International Tolerances and Maximum Residue Limits (ppm)

Commodity	U.S	Canada	Mexico
Apple	TBD	2.0	8
Avocado	0.2	8.0	
Barley, grain, postharvest	8	8.0(raw cereals)	
Bean	<i>Dry, 2.0</i> <i>Succulent, 2.0</i>	2.0	8
Blackberry	6	8.0	
Blueberry	8	8.0	
Carrot, roots	1	0.5	8
Cherry	3.0	6.0	
Corn, grain, postharvest	8.0	8.0	
Corn, sweet, kernel plus cod with husks removed	0.1		
Cucumber	0.2	3.0	8
Eggplant	2.0	0.5	8
Garlic	1.0	0.5	8
Grape	4.0	8.0	8
Melon	1.0	8.0	8
Nut, macadamia	0.2		
Papaya	1	8.0	1
Peach	6.0	6.0	8
Pear	3.0	2.0	8
Pepper	0.5	0.5	8
Potato	0.1	0.5	8
Pumpkin	1.0	3.0	8
Radish	0.5	0.5	8
Rice, grain, postharvest	30	8.0 (raw cereals)	8
Shallot, bulb	6.0		
Squash, summer and winter	<i>Summer, 0.2</i> <i>Winter, 1.0</i>	3.0 3.0	8 (zucchini)
Sweet potato, roots	0.1		
Tomato	2.0	3.0	8
Turnip (including tops)	<i>Tops, 4.0</i> <i>Roots, 0.5</i>	0.5	

TBD = To be determined

## 2.4 Conclusions

For bienzyme system, sensitive detection of OPs can be performed using a coulometric microdevice with a microelectrode array and a flow channel structure. This coulometric technique, based on the inhibition of AChE, can be performed using plugs of very small volumes, minimizing consumption of expensive reagents. Rapid mixing of plugs is beneficial for reproducibility and precise measurement. Using this technique, a very low LOD of the order of nM can be achieved. AChE activity is inhibited in the presence of high concentrations of organic solvents. However, because the influential concentrations of organic solvents are several orders of magnitude higher than those of OPs, the influence of organic solvents can be neglected in analysis of OPs. This coulometric microdevice is applicable for on-site OP detection.

For mono-enzyme system, a coulometric microdevice for OPs determination was fabricated based on the inhibition of AChE. A mono-enzyme system and simplified processing of solutions in this microfluidic device can realize low cost user-friendly analysis. A linear relationship ( $R^2=0.951$ ) was observed in the OP concentration range between  $10^{-6}$  M and  $10^{-3}$  M with a 412 nM detection limit for malathion. The sufficient sensitivity and detection limit obtained demonstrates an excellent electroanalytical performance of this microdevice.

## REFERENCES

- [1] S. Andreescu, J.L. Marty (2006). Twenty years research in cholinesterase biosensors: from basic research to practical applications. *Biomol. Eng.*, 23, 1–15.
- [2] J. Diehl-Faxon, A.L. Ghindilis, P. Atanasov, E. Wilkins (1996). Direct electron transfer based tri-enzyme electrode for monitoring of organophosphorus pesticides. *Sens. Actuators B.*, 36, 448–457.
- [3] J. Wang, C. Timchalk, Y.H. Lin (2008). Carbon nanotube-based electrochemical sensor for assay of salivary cholinesterase enzyme activity: An exposure biomarker of organophosphate pesticides and nerve agents. *Environ. Sci. Technol.*, 42, 2688–2693.
- [4] S. Andreescu, A. Avramescu, C. Bala, V. Magearu, J.L. Marty (2002). Detection of organophosphorus insecticides with immobilized acetylcholinesterase-comparative study of two enzyme sensors. *Anal. Bioanal. Chem.*, 374, 39–45.
- [5] P. Mulchandani, W. Chen, A. Mulchandani (2001). Flow injection amperometric enzyme biosensor for direct determination of organophosphate nerve agents. *Environ. Sci. Technol.*, 35, 2562–2565.
- [6] S. Andreescu, L. Barthelmebs, J.L. Marty (2002). Immobilization of acetylcholinesterase on screen-printed electrodes: comparative study between three immobilization methods and applications to the detection of organophosphorus insecticides. *Anal. Chim. Acta.*, 464, 171–180.
- [7] R. Solna, E. Dock, A. Christenson, M. Winther-Nielsen, C. Carlsson, J. Emnéus, T. Ruzgas, P. Skládal (2005). Amperometric screen-printed biosensor arrays with immobilised oxidoreductases and cholinesterases. *Anal. Chim. Acta.*, 528, 9–19.



- [8] G. Jeanty, A. Wojciechowska, J.L. Marty, M. Trojanowicz (2002). Flow-injection amperometric determination of pesticides on the basis of their inhibition of immobilized acetylcholinesterases of different origin. *Anal. Bioanalytical. Chem.*, 373, 691–695.
- [9] Y. Lin, F. Lu, J. Wang (2004). Disposable carbon nanotube modified screen-printed biosensor for amperometric detection of organophosphorus pesticides and nerve agents. *Electroanalysis*, 16, 145–149.
- [10] A. Crew, D. Lonsdale, N. Byrd, R. Pittson, J.P. Hart (2011). A screen-printed, amperometric biosensor array incorporated into a novel automated system for the simultaneous determination of organophosphate pesticides. *Biosens. Bioelectron.*, 26, 2847–2851.
- [11] A. Ciucu, C. Negulescu, R. P. Baldwin (2003). Detection of pesticides using an amperometric biosensor based on ferophthalocyanine chemically modified carbon paste electrode and immobilized bienzymatic system. *Biosens. Bioelectron.*, 18, 303–310.
- [12] S. Wu, L. Zhang, L. Qi, S. Tao, X. Lan, Z. Liu, C. Meng (2011). Ultra-sensitive biosensor based on mesocellular silica foam for organophosphorous pesticide detection. *Biosens. Bioelectron.*, 26, 2864–2869.
- [13] P.D. Patel (2002). Biosensors for measurement of analytes implicated in food safety: a review. *TrAC, Trends Anal. Chem.*, 21, 96–115.
- [14] X. Llopis, M. Pumera, S. Alegret, A. Merkoci (2009). Lab-on-a-chip for ultrasensitive detection of carbofuran by enzymatic inhibition with replacement of enzyme using magnetic beads. *Lab Chip*. 9, 213–218.
- [15] A. Arora, G. Simone, G.B. Salieb-Beugelaar, J.T. Kim, A. Manz (2010). Latest developments in micro total analysis systems. *Anal. Chem.*, 82, 4830–4847.

- [16] C. Cakal, J.P. Ferrance, J.P. Landers, P.C. Caglar (2010). Development of a micro-total analysis system ( $\mu$ -TAS) for the determination of catecholamines. *Anal. Bioanal. Chem.*, 398, 1909–1917.
- [17] W. Joseph (2004). Microchip devices for detecting terrorist weapons. *Anal. Chim. Acta.*, 507, 3–10.
- [18] K. Ohno, K. Tachikawa, A. Manz (2008). Microfluidics: applications for analytical purposes in chemistry and biochemistry. *Electrophoresis*, 29, 4443–4453.
- [19] P.S. Dittrich, K. Tachikawa, A. Manz (2006). Micro total analysis systems. Latest advancements and trends. *Anal. Chem.*, 78, 3887–908.
- [20] A. Fernández-la-Villa, D. Sánchez-Barragán, D.F. Pozo-Ayuso, M. Castaño-Álvarez (2012). Smart portable electrophoresis instrument based on multipurpose microfluidic chips with electrochemical detection. *Electrophoresis*, 33, 2733–2742.
- [21] J. Wang, H. Suzuki, and T. Satake (2014). Coulometric microdevice for organophosphate pesticide detection. *Sens. Actuators B.*, 204, 297-301.
- [22] S. Andreescu, L. Barthelmebs, J.L. Marty (2002). Immobilization of acetylcholinesterase on screen-printed electrodes: methods and applications to the detection of organophosphorus insecticides. *Anal. Chim. Acta.*, 464, 171-180.
- [23] F. M. Raushel (2011) Chemical biology: Catalytic detoxification. *Nature*, 469, 310-311.
- [24] F. Sassa, H. Laghzali, J. Fukuda, H. Suzuki (2010). Coulometric detection of components in liquid plugs by microfabricated flow channel and electrode structures. *Anal. Chem.*, 82, 8725–8732.
- [25] H. Suzuki, T. Taura (2001). Thin-film Ag/AgCl structure and operational modes to realize long-term storage. *J. Electrochem. Soc.*, 148, 468–474.

- [26] H. Song, D. L. Chen, R.F. Ismagilov (2006). Reactions in droplets in microfluidic channels. *Angew. Chem. Int. Ed.*, 45, 7336–7356.
- [27] K. A. Joshi, J. Tang, R. Haddon, J. Wang, W. Chen, A. Mulchandani (2005). Determination of organophosphate pesticides at a carbon nanotube/organophosphorus hydrolase electrochemical biosensor. *Electroanalysis*, 17, 54-58.
- [28] <http://www.epa.gov/pesticides/reregistration/REDS/malathion-red-revised.pdf>
- [29] P. Mulchandani, A. Mulchandani, I. Kaneva, W.Chen (1999). Biosensor for direct determination of organophosphate nerve agents. 1. Potentiometric enzyme electrode. *Biosens. Bioelectron.*, 14, 77-85.

## CHAPTER 3

### Microfabricated pH Sensing Device for the Direct Determination of Organophosphate Pesticide

#### 3.1 Introduction

For the detection of organophosphate pesticides (OPs), biosensing techniques such as those based on electrochemical measurement of acetylcholinesterase (AChE) inhibition provide a rapid, simple, and reliable alternative to conventional methods [1-4]. However, these biosensors need tedious protocols that require time-consuming incubation with OPs prior to the analysis. Furthermore, AChE is inhibited by other neurotoxins such as carbamate pesticides and nerve gases for chemical warfare. PON1, a family of organophosphorus hydrolase (OPH), has been shown to hydrolyze OPs such as parathion, methyl parathion, and diazinon and release protons. The concentration is proportional to the amount of OP [5], which means that the detection is more direct compared with the method that measures the degree of inhibition of AChE activity. The detection scheme based on monitoring the PON1-catalysed hydrolysis products of OPs offer the advantages in simplicity, quick, and more direct measurements of OPs over that based on the inhibition of AChE activity.

A couple of potentiometric biosensors for the direct detection of OPs were reported [6,7]. However, these biosensors consumed large amounts of reagents, because conventional glass pH electrodes were used for the measurement. To solve this problem, metal oxide electrodes, particularly iridium oxide ( $\text{IrO}_x$ ) electrode, will be more advantageous. Several techniques have been developed to form  $\text{IrO}_x$  including electrochemical growth, thermal oxidation, and sol-gel processes [6-8]. Electrochemical growth exhibits super-Nernstian

potential response to pH ranging from 60-90 mV/pH but suffers potential drift [9]. Thermal oxidation provides more stable potentials. However, the surface contains many cracks [10]. The sol-gel processes formed by dip-coating need complicate long time protocol [11]. On the other hand, IrO<sub>x</sub> formed by oxygen plasma treatment is one of the most promising materials for pH measurement, because they feature fast response with less potential drift, and excellent stability and durability [6].

In this study, we describe direct OP determination using a micro IrO<sub>x</sub> pH sensor formed by oxygen plasma treatment. The IrO<sub>x</sub> electrode can be microfabricated and can realize reliable performance in pH sensing with low cost and robustness. This pH sensor offered sensitive, stable, and rapid potential measurement during the hydrolysis of OPs.

## **3.2 Materials and methods**

### **3.2.1 Reagents and materials**

The reagents and materials used for the fabrication and characterization of the device were obtained from the following commercial sources: Glass wafers (#7740, 3-in. diameter, 500- $\mu$ m thickness) from Corning Japan (Tokyo, Japan); thick-film photoresist, SU-8 25, from Microchem (Newton, MA, USA); and prepolymer solution of polydimethylsiloxane (PDMS), KE-1300T, from Shin-Estu Chemical (Tokyo, Japan). Diazinon was purchased from Sumitomo Chemical Garden Products (Tsukuba, Japan). Agarose and paraoxonase 1 (PON1) was purchased from Sigma-Aldrich (Tokyo, Japan). A 50 mM phosphate buffer solution (PBS) (pH 7.4) was used to dissolve PON1.

### **3.2.2 Device fabrication**

The device was constructed with a glass substrate with electrodes formed by photolithography and lift-off processes and a PDMS substrate formed by replica molding

(Fig. 3.1). The dimensions of the device were 11 mm × 20 mm. The electrodes formed on the glass substrate were an IrO<sub>x</sub> indicator electrode (diameter 4 mm), an Ag/AgCl reference electrode (diameter 3.4 mm), and a concentric Au auxiliary electrode (diameter 4 mm). The auxiliary electrode was used to grow AgCl in the silver layer of the reference electrode during the use of the device. The iridium thin film is very brittle. Therefore, a gold/chromium layer was used as a base layer to form the iridium layer along with the other metal layer for the other electrodes [5,12]. The IrO<sub>x</sub> was formed on the surface of the iridium pattern in oxygen plasma. The plasma chamber was initially evacuated after which the oxidation was performed in pure oxygen at 100 W for 1 min. Five pinholes of 40 μm in diameter were formed on the silver layer of the reference electrode. AgCl was grown continuously by applying 50 nA with respect to a commercial liquid-junction Ag/AgCl reference electrode for 20 min in a 0.1 M KCl solution. The pinholes used in the Ag/AgCl electrodes showed a 20-fold increase in lifespan compared with that of conventional structures [14]. Structures in PDMS were formed with the thick-film photoresist (SU-8) template by replica molding. Two chambers were formed and connected with a liquid junction. The liquid junction was made by filling the chamber with an electrolyte gel consisting of saturated KCl and 1% agarose. The compartment for the Ag/AgCl reference electrode was also filled with saturated KCl during measurement.

The detailed fabrication procedure is described as below based on MEMS technique and standard photolithography.

### **(1) Fabrication of the on chip electrode (Fig. 3.2)**

#### Cleaning of glass substrate

First, prepare the washing solution (25% NH<sub>3</sub>·H<sub>2</sub>O: 30% H<sub>2</sub>O<sub>2</sub>: deionized water = 1 : 1 : 4) and boil it. Then, immerse the glass substrate into the boiled washing solution and

boiled deionized water in sequence for 5 min, respectively. After that, wait the glass substrate dry by itself.

#### Sputtering of Cr/Au for pH-sensing device

For pH sensing device, sputter the Cr layer for 5 min and then etched by Cr etching solution; then sputter Au layer for 12min and etched by Au etching solution.

#### Formation of Ag lift-off pattern for the device

Spin coat the positive photoresist (S1818G) again (500 rpm, 5 s → 2000 rpm, 10 s) and bake the glass substrate in the 80 °C dry oven for 30 min. Then, form the Ag lift-off pattern on the glass substrate with the designed mask by being exposed under ultra violet emitted by mask aligner for 1 min. After that, immerse the glass substrate in the 30 °C toluene for 30 s and bake it in the 80 °C dry oven for 15 min. Finally, develop the glass substrate in the positive photoresist developer for 1 min, rinse it with deionized water and dry it with N<sub>2</sub> gas.

#### Sputtering of Ag for the device

For pH-sensing device, sputter the Ag layer on the glass substrate by sputtering machine twice, each time for 12min. The output power was also set at 100 W during the sputtering process.

#### Lift-off of Ag layer for the device

Immerse the sputtered glass substrate in the acetone for at least 1 h. Then, peel the Ag layer where does not cover the electrode region from the glass substrate. Finally, wash the glass substrate again with acetone and dry it with N<sub>2</sub> gas.

### Sputtering of Ir layer for pH-sensing device

For pH-sensing device, sputter the Ir layer on the glass substrate by sputtering machine for 10 min. The output power was also set at 100 W during the sputtering process.

### Formation of insulating layer

Spin coat the insulating layer (polyimide layer), polyimide (500 rpm, 10 s → slope, 5 s → 4000 rpm, 30 s) on the Pt/Cr/Ag and Cr/Au/Ag/Ir patterned glass substrate and bake the glass substrate in the 80 °C dry oven for 30 min, respectively.

### Formation of positive photoresist layer

Spin coat positive photoresist (S1818G) on the glass substrate (500 rpm, 5 s → 2000 rpm, 15 s) and bake it in the 80 °C dry oven for 30 min.

### Formation of insulating layer pattern

Form the insulating layer, polyimide pattern mask were used under the ultra violet emitted for exposure by mask aligner for 1 min. Then, immerse the glass substrate in the positive photoresist developer for 1 min. Finally, immerse the glass substrate in the ethanol and strip off the positive photoresist layer.

### Cure of insulating layer

Put the glass substrate on the hot plate and cover it (150 °C, 15 min → 200 °C, 15 min → 280 °C, 30 min) for curing the insulating layer, polyimide.



### Dicing

Spin coat positive photoresist (S1818G) (500 rpm, 15 s → 2000 rpm, 15 s) on the glass substrate for protecting the on chip electrode during the dicing and bake the glass substrate in the 80 °C dry oven for 30 min. Then, immobilize the glass substrate on the immobilization sheet. Finally, cut the glass substrate into devices one by one and rinse the protection layer with acetone and deionized water. The size of was 20 mm × 11 mm for pH-sensing device.

### Formation of Ag/AgCl layer (Fig. 3.3)

Two pinholes of 30 μm in diameter for coulometric device and five pinholes of 50μm in diameter were formed on the silver layer of the reference electrode, where AgCl was grown by applying a current of 50 nA for 20 min in a 0.1 M KCl solution.

### Formation of Ir/IrOx layer for pH-sensing device (Fig. 3.4)

Iridium oxide was formed on the surface of the iridium pattern in oxygen plasma. The plasma chamber was initially evacuated after which the oxidation was performed in pure oxygen at a RF generator 100 W for 1 min. At all times the substrate temperature was maintained at relatively low.

## **(2) Fabrication of PDMS substrate**

### Cleaning glass substrate

First, prepare and boil the washing solution (25% NH<sub>3</sub>·H<sub>2</sub>O : 30% H<sub>2</sub>O<sub>2</sub> : deionized water = 1 : 1 : 4). Then, immerse the glass substrate into the boiled washing solution and boiled deionized water in sequence for 5 min, respectively. After drying, put the substrate

in the oxygen plasma chamber for plasma cleaning for 1 min. The output power was set at 100 W during the plasma cleaning.

#### Formation of SU-8 pattern

Spin coat SU-8 (500 rpm, 5 s → 2000 rpm, 15 s) onto the glass substrate. Additionally, put a more than 3 g SU-8 on the glass substrate after spin coat. Then, put the glass substrate on the hot plate with a cover at 65 °C and 95 °C for 10 min and 8 h, respectively. After that, form the mask for higher part SU-8 pattern was used for exposure for 480 s. Finally, bake the glass substrate again on the hot plate at 65 °C for 20 min.

#### Developing of SU-8

Develop and rinse SU-8 in the SU-8 developer. Clean the glass substrate in 2-propanol to get rid of contamination. Then, dry with N<sub>2</sub> gas.

As far as, the SU-8 template was finished. The PDMS substrate for the device was carried out based on the SU-8 template.

#### Preparation of PDMS substrate for both devices

Mix the precursor solution of PDMS (KE-1300T) and curing solution (CAT-1300) with a mass ratio of 10 : 1. Then, pour the mixture on the surface of the SU-8 template uniformly and vacuumed it to get rid of foam in a vacuum pump. After that, cure the PDMS in the 80 °C dry oven for 30 min and strip off it from SU-8 template. Finally, cut the PDMS into pieces one by one according to the design dimensions.

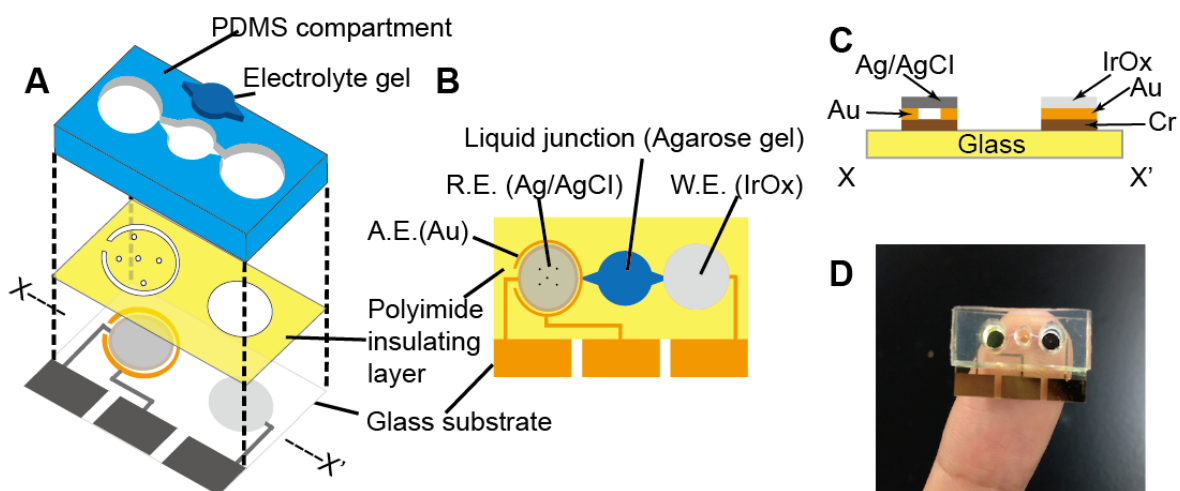


Fig. 3.1 Construction of the device. A: Exploded view of the device. B: Top view showing the mutual relation between the structures of the layers. C: Cross-section along the line X-X' in A. D: The device on a finger. Planar dimensions are 20 mm × 11 mm.

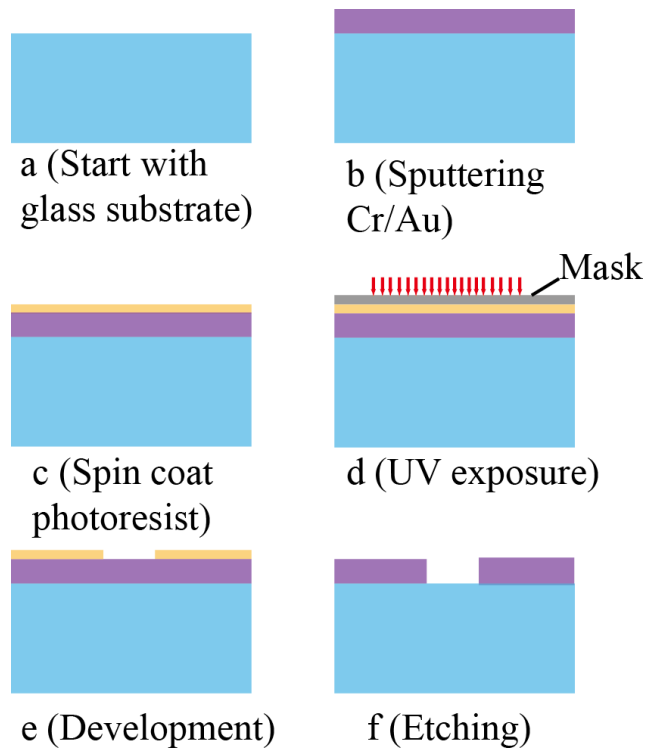


Fig. 3.2 Schematic illustration of the fabrication of on chip electrode for pH-sensing device.

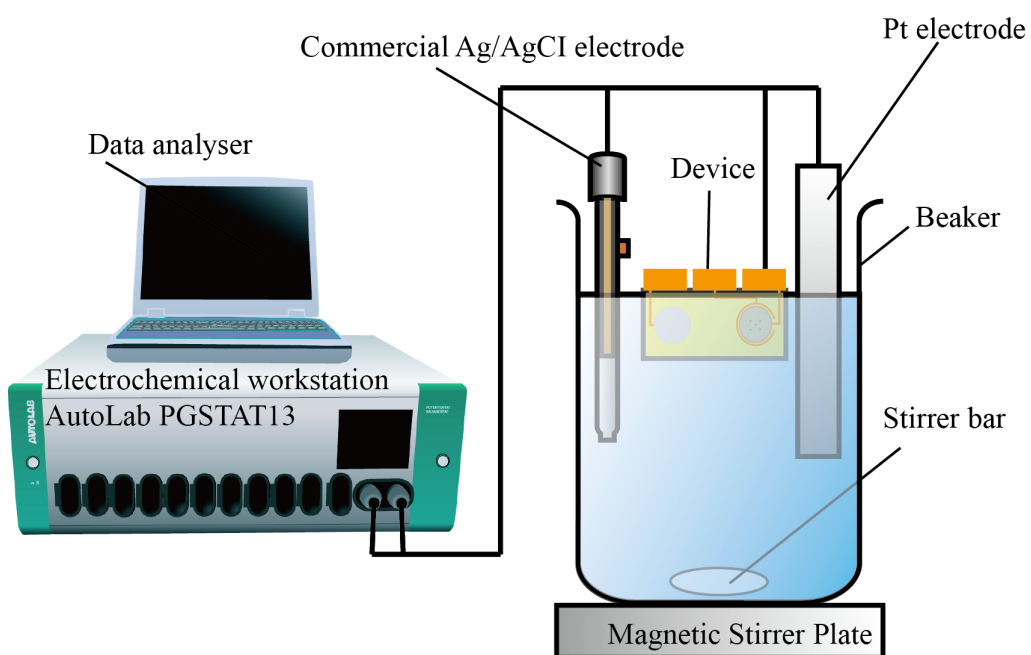


Fig. 3.3 Schematic illustration formation of Ag/AgCl layer on the device.

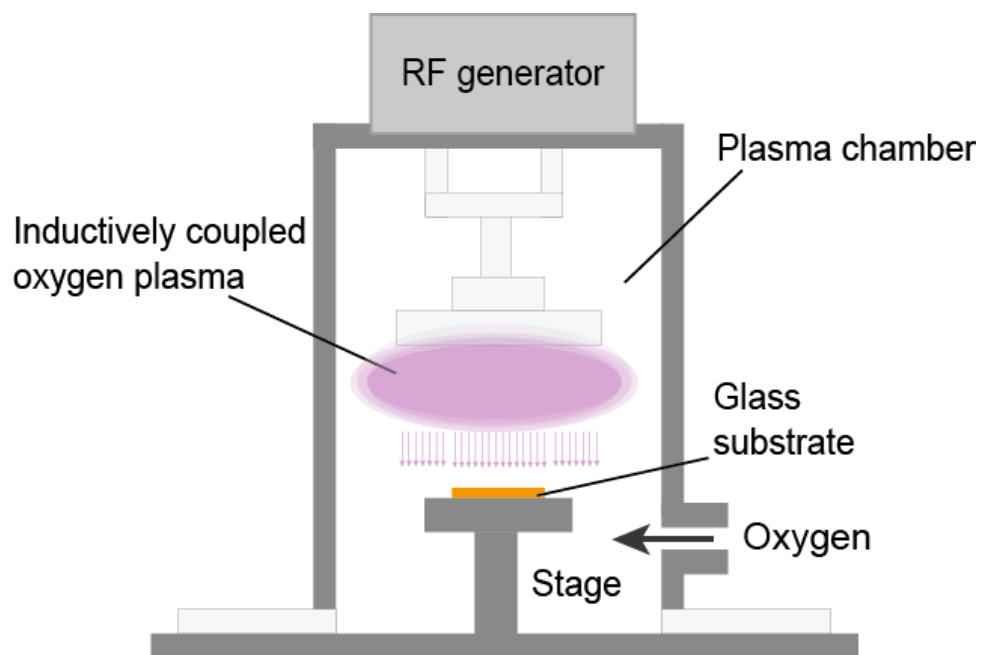


Fig. 3.4 Formation of Ir/IrOx layer for pH-sensing device

### 3.2.3 Measurement procedure

An electrochemical workstation (Autolab PGSTAT13, Eco Chemie, Utrecht, The Netherlands) connected to a personal computer was used to characterize the device. The pH values and potentials were recorded and displayed in the computer. The response of the pH sensor was examined with buffer solutions and diluted acids and bases. The pH values of the solutions were adjusted by adding hydrochloric acid or sodium hydroxide and were checked using a commercial pH meter (Mettler-Toledo, SevenCompact™ S220). After each measurement, the pH electrode chamber was washed thoroughly with distilled water twice. The on-chip Ag/AgCl reference electrode was used with or without applying a constant current (50 nA). The current value was decided so as not to polarize the Ag/AgCl electrode. The experiments were conducted at room temperature.

## 3.3 Results and Discussion

### 3.3.1 Performance characterization of the IrOx electrode

As for the equilibrium on the IrO<sub>x</sub> electrode, three mechanisms are possible [7].



For all cases, the relation between the potential and pH is described by the same Nernst equation

$$E = E^0 - 2.303 \frac{RT}{F} \text{pH} = E^0 - 0.05916 \text{pH} \quad (3-4)$$

at 25°C. Where E is the potential of the pH electrode (mV), E<sup>0</sup> is the standard electrode potential, R is the gas constant, T is the absolute temperature, F is the faraday constant.

The sensitivity of the IrO<sub>x</sub> pH sensor was examined by injecting solutions (20 μL) of different pHs into the PDMS chamber. After each measurement, the chamber was washed twice with distilled water to eliminate residue of the previous solution. A near-Nernstian response (60.6±0.8 mV/pH) was observed with a correlation coefficient R<sup>2</sup> of 0.997 (Fig. 3.5). Compared with other previously reported metal oxide electrodes including a PbO<sub>2</sub> electrode (57.9 mV/pH) [16], a SnO<sub>2</sub> electrode (46.6 mV/pH), a RuO<sub>2</sub> electrode (61.8 mV/pH), a Ta<sub>2</sub>O<sub>5</sub> electrode (49.3 mV/pH), and a TiO<sub>2</sub> electrode (55.0 mV/pH) [15,17], the sensitivity of our IrO<sub>x</sub> electrode is close to that anticipated from eq. (4). Furthermore, as shown in Fig. 3.6, a smooth potential change without damped oscillation or over-shooting was observed as shown in Fig. 3.7. The 90% response time was less than 2 s.

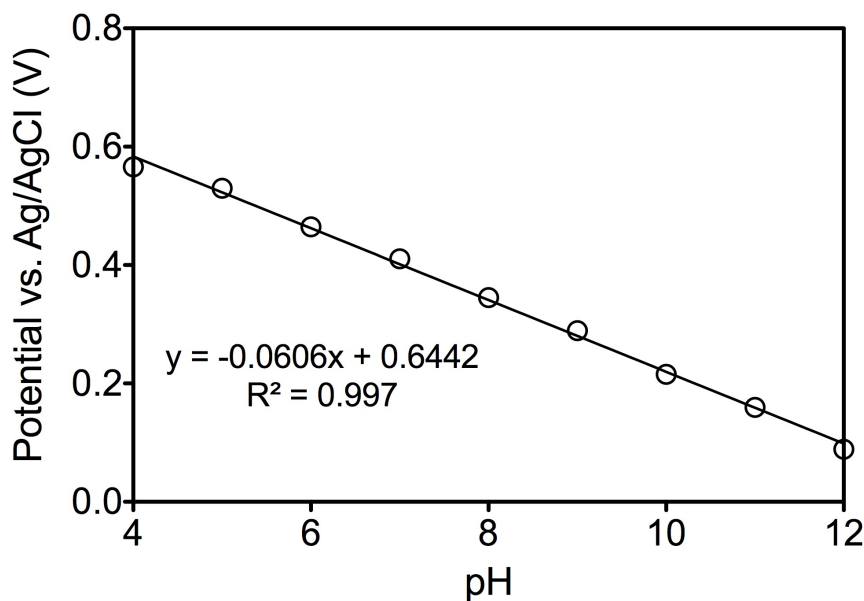


Fig. 3.5 Calibration plot for the IrO<sub>x</sub> pH electrode obtained using the on-chip liquid junction Ag/AgCl reference electrode. Eight measurements were done for each point, and averages and standard deviations are shown. All of the error bars are behind the symbols.



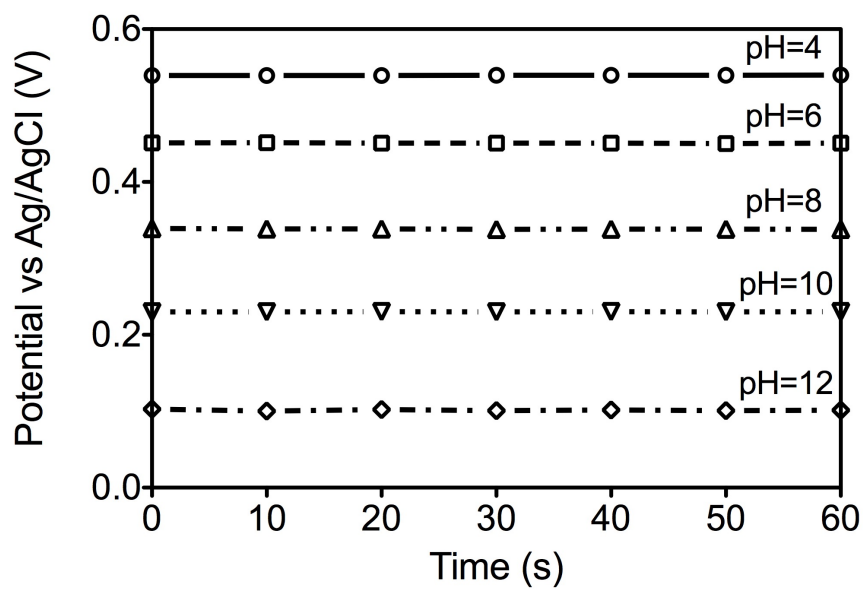
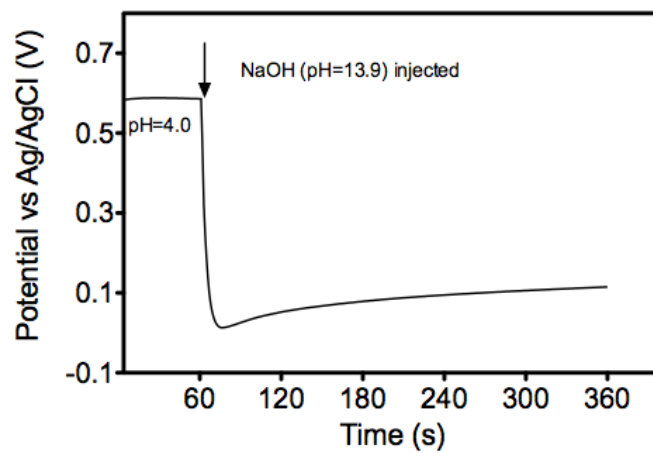


Fig. 3.6 Stability of the IrO<sub>x</sub> electrode in solutions of different pH values. Each data point represents the average of four measurements; averages and standard deviations are shown. Most of the error bars are behind the symbols.

A



B

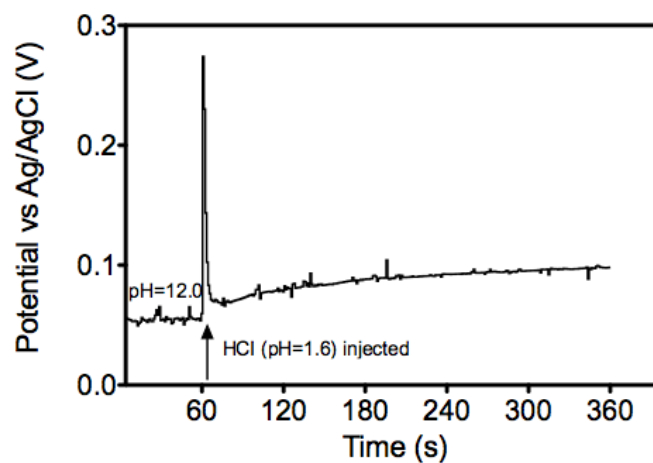


Fig. 3.7 Response curves of the IrO<sub>x</sub> electrode to pH changes.

A: Adding a NaOH solution to a HCl solution (pH 1.6),

B: adding a HCl solution to a NaOH solution (pH 13.9).

### 3.3.2 Potentiometric determination of diazinon

#### 3.3.2.1 Effect of buffer pH on PON1

The pH profile for the OPH-immobilized enzyme electrode and free enzyme are similar [4]. In this work, the free enzyme is applied for diazinon detection. The pH=7.4 and pH = 8.0 buffer solution was used for preparation of enzyme solutions, respectively. As the results shown in the Fig. 3.8, pH 7.4 gave the maximum activity of PON1 and the response was significantly increased over that in pH 8.0.

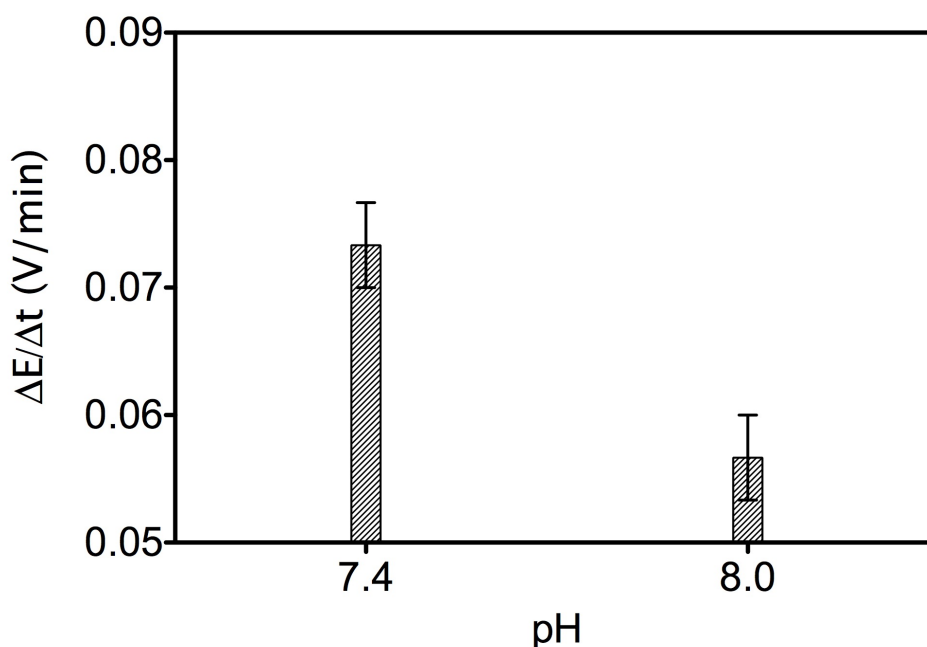


Fig. 3.8 Response of starting buffer pH on PON1 electrode to 0.1 mM diazinon.

### 3.3.2.2 Precision and accuracy of the micro pH sensor

The low relative standard deviation of 1.06 % (n = 30) in the response of .1mM diaznion sample was observed in the Fig. 3.9, demonstrating an excellent reproducibility and reliable during the measurements, which agreed with former reports that the good agreement between spectrophotometric method and enzyme electrode [4].

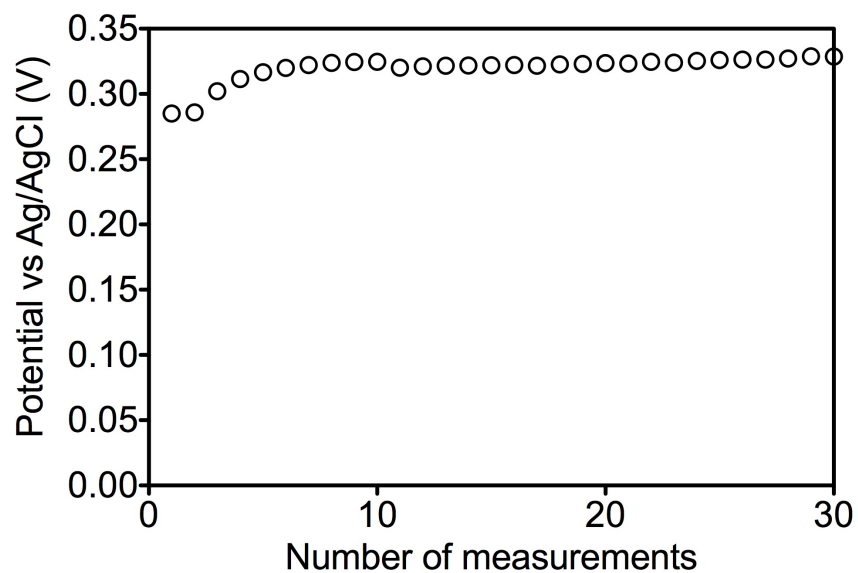


Fig. 3.9 Reproducibility of the PON 1 IrOx electrode at 0.1 mM diazinon.

#### 3.3.2.4 Selectivity

Different from the AChE inhibited biosensors, the present micro sensor is highly special for organophosphate pesticides. Other widely used pesticides, malathion, acephate, MEP at 0.1mM concentrations do not interfere (Table 3.1). That is a significant advantage over the AChE inhibited biosensors.

Table 3.1 Response of the potentiometric electrode to other pesticides

Pesticide	Concentration, mM	Response, V
Malathion	0.1	0
Acephate	0.1	0
MEP	0.1	0

### 3.3.2.5 Direct determination of diazinon

Direct determination of diazinon was based on measurement of a pH change caused by the enzymatic reaction. PON 1 catalyses the hydrolysis of diazinon to release  $H^+$ , and the accompanying pH change can be monitored using the  $IrO_x$  electrode. The results shown in Fig. 3.10 demonstrate that a linear relationship was observed in a range between 50 and 100  $\mu M$  ( $R^2 = 0.939$ ). The lower detection limit was 2.5  $\mu M$ . Table 3. 2 showed the Limit of direct detection of OP biosensors for various OPs based on direct determinaiton. Although, this detection limit is one to three orders of magnitude higher than that based on the measurement of the inhibition of AChE inhibited biosensors, it is sufficient to detect diazinon of the concentrations of this order according to the requirements of maximum residue level (MRLs). Furthermore, our device will be ideal for selectively monitoring only the organophosphate-based pesticides with consuming very few volumes of solutions.

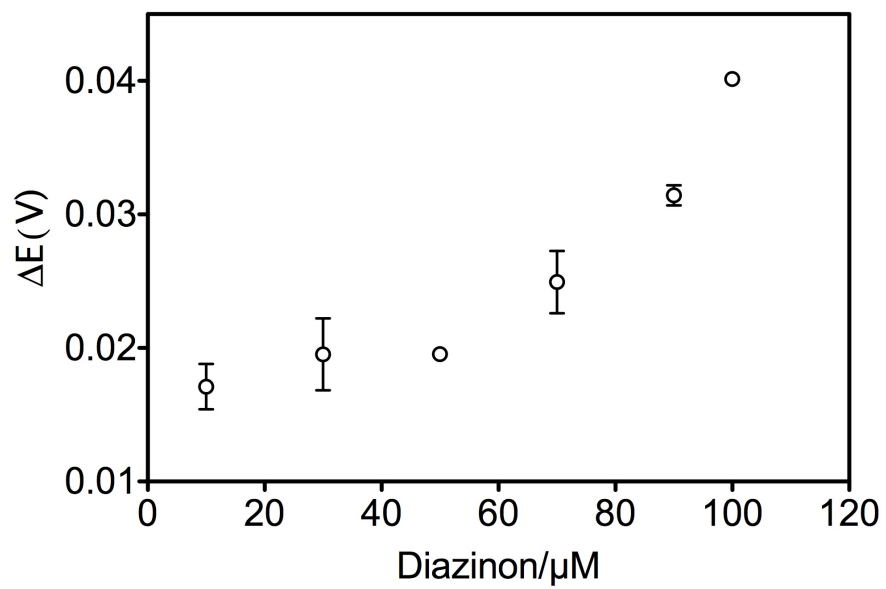


Fig. 3.10 Calibration plots for organophosphate pesticide (diazinon).

Table 3.2 Limit of direct detection of OP biosensors for various OPs.

OPs	Enzyme	Electrochemical Method	LOD	References
Diazinon	PON1	Potentiometric	2.5 $\mu$ M	This work
Dichlofenthion	Mutant OPH	Amperometric 0.050V vs. Ag/AgCl	24 $\mu$ M	[18]
Methyl Parathion	OPH	Amperometric 0.90V vs. Ag/AgCl	0.8 $\mu$ M	[19]
Paraoxon	OPH	Amperometric 0.75 V vs. Ag/AgCl	0.1 $\mu$ M	[20]
Methyl Parathion	OPH	Amperometric 0.9V vs. Ag/AgCl	1 $\mu$ M	[21]
Paraoxon	OPH	Potentiometric	5 $\mu$ M	[22]
Chlorpyrifos	OPH	Potentiometric	5 $\mu$ M	[22]
Diazinon	OPH	Potentiometric	5 $\mu$ M	[4]
Paraoxon	OPH	Potentiometric	2 $\mu$ M	[4]
Parathion	OPH	Potentiometric	2 $\mu$ M	[4]
Methyl parathion	OPH	Potentiometric	2 $\mu$ M	[4]

### 3.4 Conclusions

A microfabricated pH-sensing device with an IrO<sub>x</sub> indicator electrode was used for direct determination of an organophosphate pesticide, diazinon based on different detection mechanism for organophosphate pesticides. The pH-sensing IrO<sub>x</sub> electrode formed in oxygen plasma showed stable and reproducible responses with a sensitivity close to that anticipated from the Nernst equation. The electrode incorporated in a PDMS chamber can be used for direct determination diazinon. The system only needs one-step reaction. PON1 was used for the hydrolysis reaction and the final detection signal proton released during the hydrolysis reaction was measured by a sensitive IrO<sub>x</sub> electrode. Different from the bienzymes and mono-enzyme system detection, also called indirect detection, the pH-sensing device is direct detection of OPs. The lower detection limit was 2.5 μM and this method clarified the feasibility of this micro device for the first screening detection of organophosphate pesticides with high sensitivity.



## REFERENCES

- [1] S. Andreescu, L. Barthelmebs, J.L. Marty (2002). Immobilization of acetylcholinesterase on screen-printed electrodes: comparative study between three immobilization methods and applications to the detection of organophosphorus insecticides. *Anal. Chim. Acta.*, 464, 171–180.
- [2] A. Crew, D. Lonsdale, N. Byrd, R. Pittson, J.P. Hart (2011). A screen-printed, amperometric biosensor array incorporated into a novel automated system for the simultaneous determination of organophosphate pesticides. *Biosens. Bioelectron.*, 26, 2847–2851.
- [3] J. Wang, H. Suzuki, and T. Satake (2014). Coulometric microdevice for organophosphate pesticide detection. *Sens. Actuators B.*, 204, 297–301.
- [4] P. Mulchandani, A. Mulchandani, I. Kaneva, W. Chen (1999). Biosensor for direct determination of organophosphate nerve agents. 1. Potentiometric enzyme electrode. *Biosens. Bioelectron.* 14, 77–85.
- [5] C.H. Chen, K.L. Yang. (2013). A liquid crystal biosensors for detecting organophosphates through the localized pH changes induced by their hydrolytic products. *Sens. Actuators B.*, 181, 368–374.
- [6] M. Wang, S. Yao, M. Madou (2002). A long-term stable iridium oxide pH electrode. *Sens. Actuators B.*, 81, 313–315.
- [7] W.D. Huang, H. Cao, S. Deb, M. Chiao, J.C. Chiao (2011). A flexible pH sensor based on the iridium oxide sensing fillm. *Sens. Actuators A.*, 169, 1–11.

- [8] T.Y. Kim, S. Yang (2014). Fabrication method and characterization of electrodeposited and heat-treated iridium oxide films for pH sensing. *Sens. Actuators B.*, 196, 31–38.
- [9] K. Yamanaka (1989). Anodically electrodeposited iridium oxide films (AEIROF) from alkaline solutions for electrochromic display devices. *Jap. J. Appl. Phys.*, 28, 632–637.
- [10] P.J. Kinlen, J.E. Heider, D.E. Hubbard (1994). A solid-state pH sensor based on a nafion-coated iridium oxide indicator electrode and a polymer-based silver chloride reference electrode. *Sens. Actuators B.*, 22, 13–25.
- [11] X.R. Huang, Q.Q. Ren, X.J. Yuan, W. Wen, W. Wen, D.P. Zhan (2014). Iridium oxide based coaxial pH ultramicroelectrode. *Electrochem. Commun.*, 40, 35–37.
- [12] K. Morimoto, M. Toya, J. Fukuda, H. Suzuki (2008). Automatic electrochemical micro-pH-stat for biocrossystems. *Anal. Chem.*, 80, 905–914.
- [13] H. Suzuki, H. Shiroishi (1999). Microfabricated liquid junction Ag/AgCl reference electrode and its application to a one-chip potentiometric sensor. *Anal. Chem.*, 71, 5069–5075.
- [14] K. Toda, Y. Yawata, E. Setoyama, J. Fukuda, N. Nomura, H. Suzuki (2011). Continuous monitoring of ammonia removal activity and observation of morphology of microbial complexes in a microdevice. *Appl. Environ. Microb.*, 77, 4253–4255.
- [15] E. Bakker (1997). Selectivity of liquid membrane ion-selective electrodes. *Electroanalysis*, 9, 7–12.
- [16] A. Eftekhari (2003). Development of the tin oxide pH electrode by the sputtering method. *Sens. Actuators B.*, 88, 234.
- [17] A. Fog, R.P. Buck (1984). Electronic semiconducting oxides as pH sensors. *Sens. Actuators*, 5, 137.

- [18] A. Sahin, K. Dooley, D.M. Cropek, A.C. West, S. Banta (2011). A dual enzyme electrochemical assay for the detection of organophosphorus compounds using organophosphorus hydrolase and horseradish peroxidase. *Sens. Actuators B.*, 158, 353-360.
- [19] R.P. Deo, J. Wang, I. Block, A. Mulchandani, K.A. Joshi, M. Trojanowicz, F. Scholz, W. Chen, Y. Lin (2005). Determination of organophosphate pesticides at a carbon nanotube/organophosphorus hydrolase electrochemical biosensor. *Analytica Chimica Acta.*, 530, 185–189.
- [20] J. Wang, R. Krause, K. Block, M. Musameh, A. Mulchandani, M.J. Schöning (2003). Flow injection amperometric detection of OP nerve agents based on an organophosphorus-hydrolase biosensor detector. *Biosensors and Bioelectronics.*, 18, 255–260.
- [21] P. Mulchandani, W. Chen, A. Mulchandani, J. Wang, L. Chen (2001). Amperometric microbial biosensor for direct determination of organophosphate pesticides using recombinant microorganism with surface expressed organophosphorus hydrolase. *Biosensors and Bioelectronics.* 16, 433–437.
- [22] S. Gaberlein, M. Knoll, C. Zaborosch, F. Spener (2000). Disposable potentiometric enzyme sensor for direct determination of organophosphorus insecticides. *The Analyst*, 125, 2274–2279.

## CHAPTER 4

### Overall Conclusions

Organophosphate pesticides (OPs), widely used in agriculture and environment, can be hydrolyzed rapidly when exposed to sunlight, air, and soil, although small amounts can be detected in food and drinking water. Even at relatively low-level residual, organophosphates pesticides may also be the most hazardous and acute toxic for food safety, public health and environmental issues. They can be absorbed by eating the vegetables and fruits or through breath or skin contact.

Electrochemical sensors and biosensors have significantly increased and become an important tool for organophosphate pesticides. With the development of the MEMS or  $\mu$ -TAS technology, the miniaturization of electrochemical sensor has made a great progress. Based on this background, in this study, we designed and fabricated two different kinds of micro electrochemical sensor for organophosphate pesticides detection.

In the first chapter, we introduced the hazardness of organophosphate pesticides on human being, animals, environment and food firstly, then summarized the development of electrochemistry technology used for pesticides detection and other field; Finally, we introduced the microfabrication technique used for a low-cost, portable, and hand-held device integration.

In the second chapter, we designed and fabricated the coulometric microdevice based on different enzyme substrate of organophosphate pesticides: one is the bienzymes system for the final electrochemical signal  $H_2O_2$  detection; the other is mono-enzyme system for the signal TCh detection. Meanwhile, the microfabrication procedure for the coulometric device was described in detail. The coulometric device in small size was finally performed on a chip platform that realized the small volume of reagents consumption and easy

operation.

In the bienzyme system, the micro coulometric device fabricated was used for organophosphate pesticides detection. Sensitive detection of OPs was observed and performed using this microdevice with a microelectrode array and a flow channel structure. The detection of OPs, based on the inhibition of AChE, was performed in the PDMS flow channel with rhombus structure, using plugs of very small volumes, minimizing consumption of expensive reagents. Rapid mixing of plugs at the T-junction structure was beneficial for reproducibility and precise measurement. Using the coulometric technique, different from amperometric and potentiometric technique, a very low LOD of the order of nM was achieved. For four OPs, the results were shown as follows. The linear range is  $10^{-10}$ – $10^{-2}$  M for malathion ( $R^2 = 0.982$ ), acephate ( $R^2 = 0.956$ ), and MEP ( $R^2 = 0.963$ ). For diazinon, the linear range was  $10^{-12}$ – $10^{-6}$  M ( $R^2 = 0.935$ ). The detection of limit for malathion was 33 nM ( $3\sigma$ ). For acephate, MEP, and diazinon, the detection limit was 90 nM ( $3\sigma$ ). Considering that the OPs from commercial formulations including some organic solvents, which also had the influence on the AChE activity, we also investigated the effects on OPs detection. The results showed that AChE activity was inhibited in the presence of high concentrations of organic solvents. However, because the influential concentrations of organic solvents were several orders of magnitude higher than those of OPs, the influence of organic solvents was neglected in analysis of OPs. Some situation still needs to be optimized when conducted the OPs detection. However, based on those results we obtained, we can make a conclusion that this coulometric microdevice is applicable for on-site OPs detection in the future.

The same coulometric microdevice was used for OPs determination for mono-enzyme system. Different from three steps reactions involving two enzymes (bienzymes) in third chapter, a two-step reaction and mono-enzyme was applied in the fourth chapter.

Introducing only one enzyme into the reaction will reduce the cost of sample consumption; besides, the sample plugs can be easily formed and transported to the electrode area for detection than bienzymes system. For malathion detection, a linear relationship ( $R^2=0.951$ ) was also observed in the OP concentration range between  $10^{-6}$  M and  $10^{-3}$  M with a 412 nM detection limit. The maximum residue level (MRL), representing the upper legal limit of the concentration of pesticide residues in food, for malathion is 0.01 - 8 ppm (30.2 nM - 24.2  $\mu$ M) according to the Japan Food Chemical Research Foundation. The sufficient sensitivity and detection limit obtained demonstrates that the mono-enzyme microfluidic microdevice can be used off-line analysis.

In the third chapter, based on different detection mechanism for organophosphate pesticides, a microfabricated pH-sensing device with an  $\text{IrO}_x$  indicator electrode was used for direct determination of an organophosphate pesticide, diazinon. The system only needs one-step reaction. PON1 was used for the hydrolysis reaction and the final detection signal proton released during the hydrolysis reaction was measured by a sensitive  $\text{IrO}_x$  electrode. Different from the bienzymes and mono-enzyme system detection, also called indirect detection, the pH-sensing device is direct detection of OPs. The lower detection limit was 2.5  $\mu$ M. Although, this detection limit is one to three orders of magnitude higher than that based on the measurement of the inhibition of AChE inhibited biosensors (indirect detection), it is sufficient to detect diazinon of the concentrations of this order according to the requirements of maximum residue level (MRLs). Furthermore, the pH-sensing  $\text{IrO}_x$  electrode formed in oxygen plasma showed stable and reproducible responses, making the easy fabrication. The microelectrode incorporated in a PDMS chamber can be integrated and used for direct determination diazinon.

In this study, two kinds of electrochemical microdevices were fabricated for organophosphate pesticides detection based on different mechanism. This study focuses on

clarifying the feasibility of these micro devices for the first screening detection of organophosphate pesticides to evaluate the food safety. Based on the results, it was cleared that the micro devices are feasible for the detection of residual pesticide as a first step. To achieve excellent application when conducting the OPs detection in real sample, more situations should be considered and the performance of the sensors need to be optimized and improved in the near future.

## ACKNOWLEDGEMENTS

This research and dissertation couldn't be accomplished if not receiving many supports. Firstly, I want to express my great thankfulness and gratitude to my two academic supervisors, Prof. Takaaki Satake, Graduate School of Life and Environmental Sciences, and Prof. Hiroaki Suzuki, Graduate School of Pure and Applied Sciences, University of Tsukuba, for their great guidance, advice, support and encouragement throughout my study. I feel so lucky that I met two great professors in Japan.

I appreciate the advice and suggestions from my committee members, Prof. Yutaka Kitamura, Prof. Seigo Sato, Assoc.Prof. Shigeki Yoshida, for their helpful guidance and valuable suggestions. I especially hope to express my gratitude and appreciation to Prof. Masatoshi Yokokawa and my friend Zhi Cai, from Graduate School of Pure and Applied Sciences, who give me many supports and guidance and helpful advice during my research. They are so kind to me when I was in trouble with my experiment. I deeply appreciate that.

I also would like to give my thanks to lab members for their kindly help and assistance to my research. I will never forget the time we spent together.

Besides, I would express my sincere appreciation to the China Scholarship Council (CSC) for providing the financial support for me to study in Doctoral Program of Graduate School of Life and Environmental Sciences, University of Tsukuba.

At last, I would also express special thanks to my parents and my elder sisters, for their encouragement and support during my stay in Japan.

2015/5

Jin WANG



## APPENDIX

The masks for the fabrication of the coulometric and pH-sensing device in this study are shown as below. All of the masks were designed based on 76.2 mm glass substrate. Adobe Illustrator CS6 was used for design of the mask.

The designed mask for coulometric device

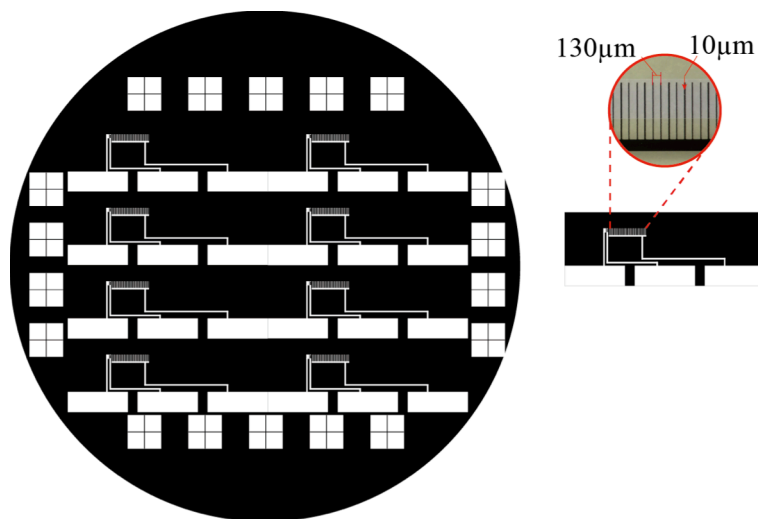
Mask 1: Cr/Pt lift-off pattern

Mask 2: Ag lift-off pattern

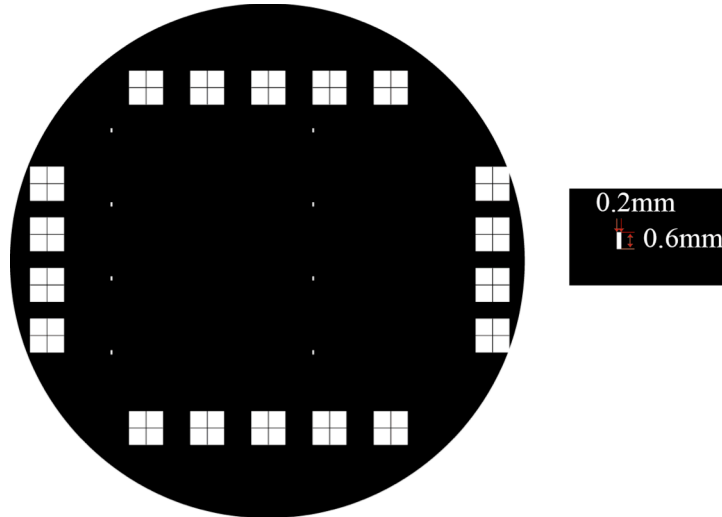
Mask 3: polyimide pattern

Mask 4: SU-8 pattern (lower part)

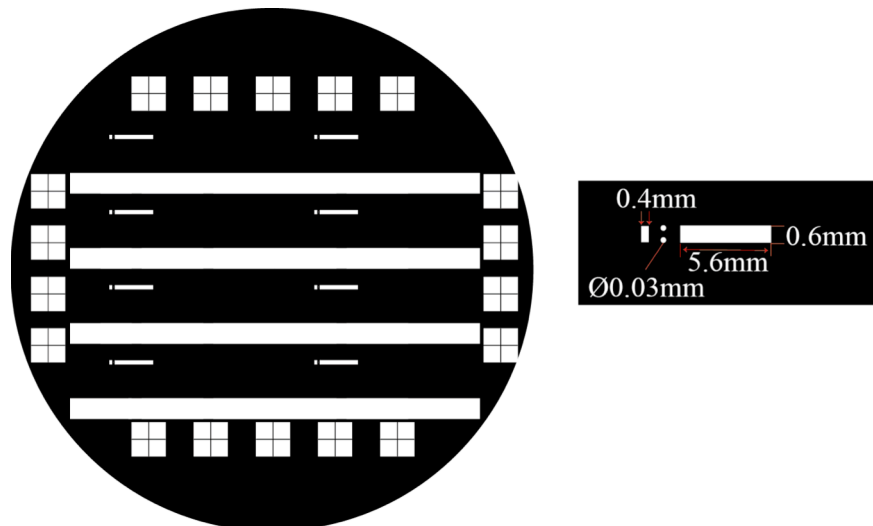
Mask 5: SU-8 pattern (higher part)



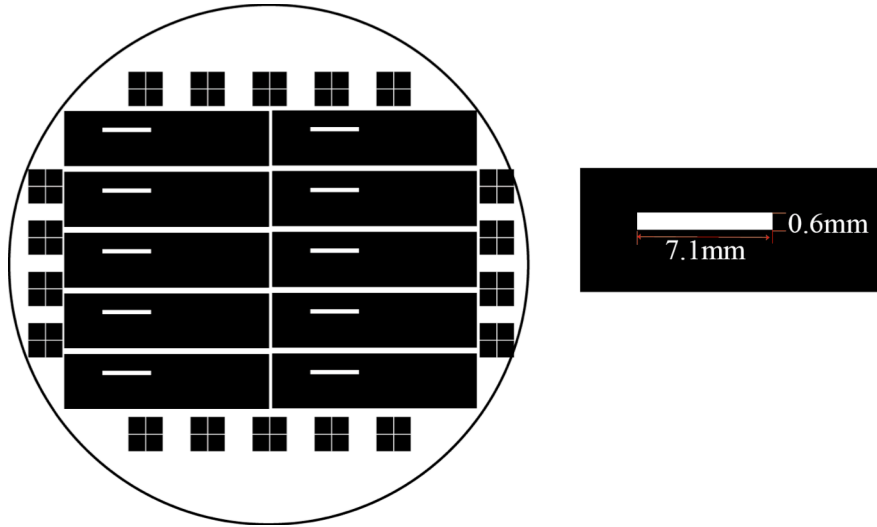
Mask 1. Cr/Pt lift-off pattern



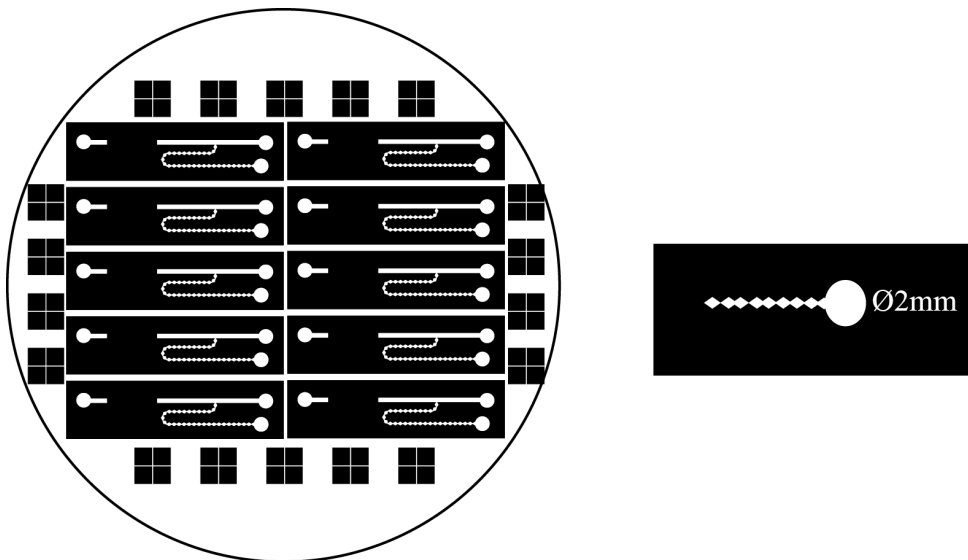
Mask 2. Ag lift-off pattern



Mask 3. Polyimide pattern



Mask 4. SU-8 pattern (lower part)



Mask 5: SU-8 pattern (higher part)

## The design mask for pH-sensing device

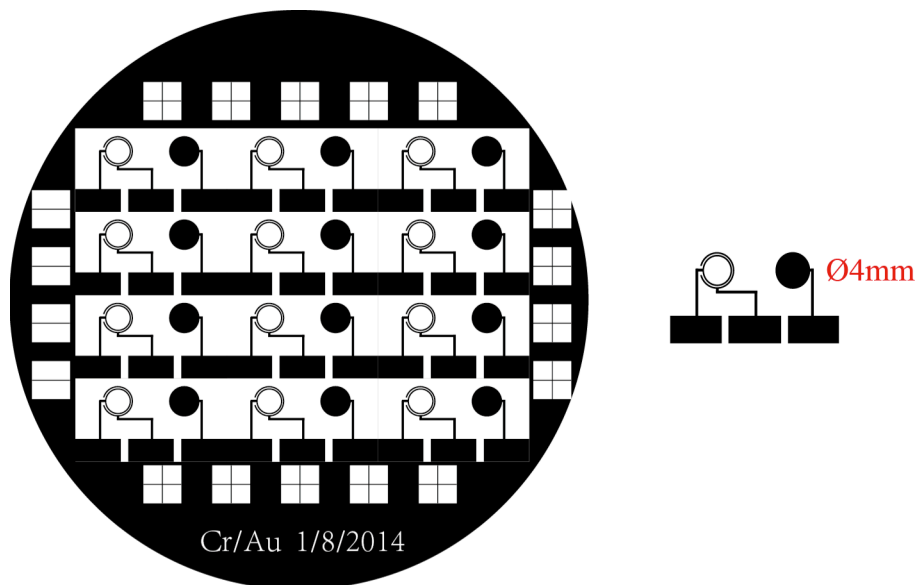
Mask 1. Cr/Au pattern

Mask 2. Ir pattern

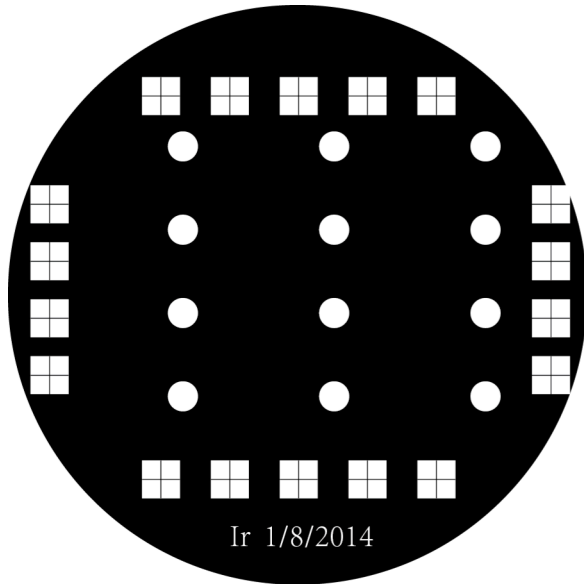
Mask 3. Ag pattern

Mask 4. Polyimide pattern

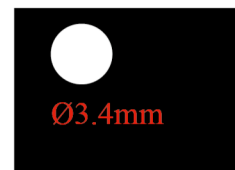
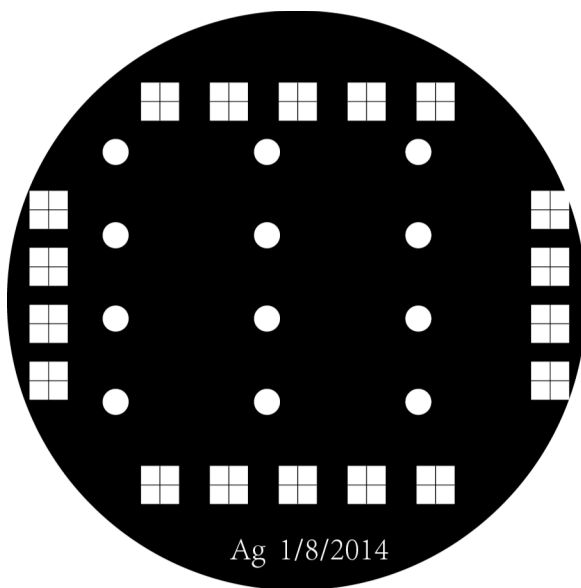
Mask 5. PDMS pattern



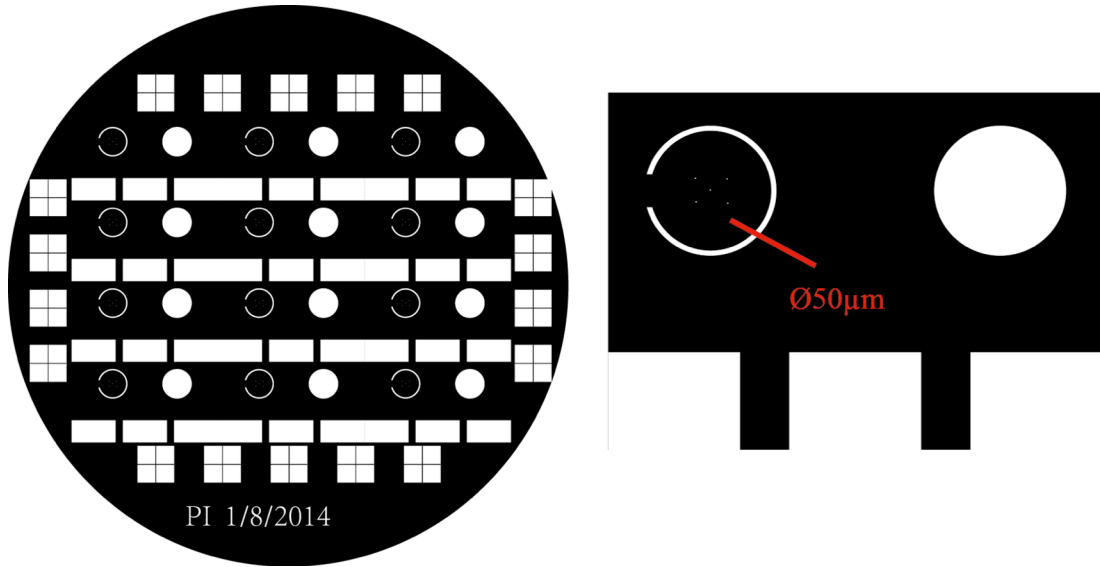
Mask 1. Cr/Au pattern



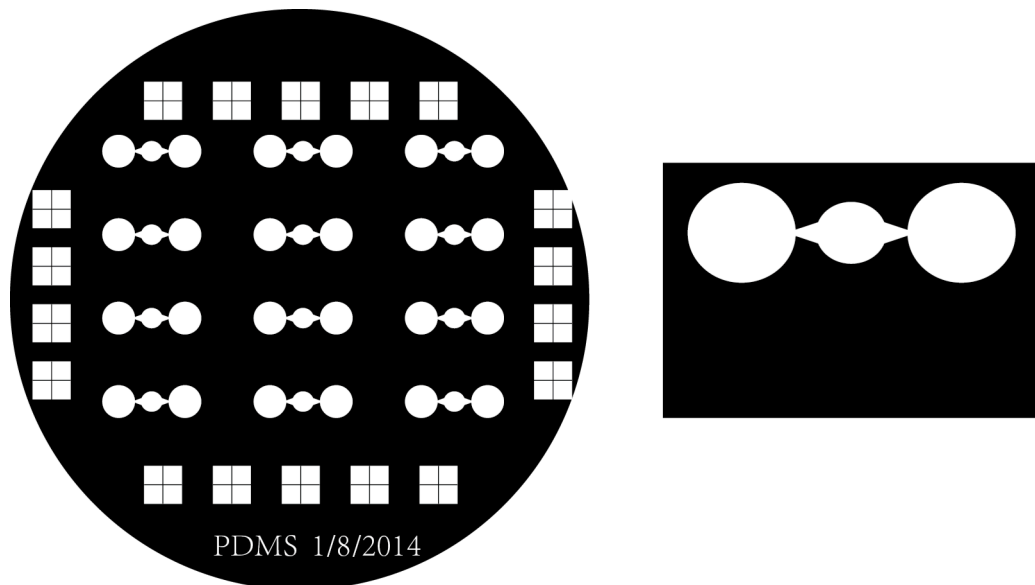
Mask 2. Ir pattern



Mask 3. Ag pattern



Mask 4. Polyimide pattern



Mask 5. PDMS pattern